



HAL
open science

PTC readthrough in human cells occurs in novel cytoplasmic foci and requires UPF proteins

Jieshuang Jia, Elisabeth Werkmeister, Sara Gonzalez-Hilarion, Catherine Leroy, Dieter C Gruenert, Frank Lafont, David Tulasne, Fabrice Lejeune

► **To cite this version:**

Jieshuang Jia, Elisabeth Werkmeister, Sara Gonzalez-Hilarion, Catherine Leroy, Dieter C Gruenert, et al.. PTC readthrough in human cells occurs in novel cytoplasmic foci and requires UPF proteins. Journal of Cell Science, 2017, 10.1242/jcs.198176 . hal-03834779

HAL Id: hal-03834779

<https://hal.science/hal-03834779v1>

Submitted on 31 Oct 2022

HAL is a multi-disciplinary open access archive for the deposit and dissemination of scientific research documents, whether they are published or not. The documents may come from teaching and research institutions in France or abroad, or from public or private research centers.

L'archive ouverte pluridisciplinaire **HAL**, est destinée au dépôt et à la diffusion de documents scientifiques de niveau recherche, publiés ou non, émanant des établissements d'enseignement et de recherche français ou étrangers, des laboratoires publics ou privés.

RESEARCH ARTICLE

Premature termination codon readthrough in human cells occurs in novel cytoplasmic foci and requires UPF proteins

Jieshuang Jia^{1,2,3,*}, Elisabeth Werkmeister^{3,4,5,6,7,*}, Sara Gonzalez-Hilarion⁸, Catherine Leroy^{1,2,3}, Dieter C. Gruenert^{9,10,§}, Frank Lafont^{5,6,7,3}, David Tulasne^{1,2,3} and Fabrice Lejeune^{1,2,3,¶}

ABSTRACT

Nonsense-mutation-containing messenger ribonucleoprotein particles (mRNPs) transit through cytoplasmic foci called P-bodies before undergoing nonsense-mediated mRNA decay (NMD), a cytoplasmic mRNA surveillance mechanism. This study shows that the cytoskeleton modulates transport of nonsense-mutation-containing mRNPs to and from P-bodies. Impairing the integrity of cytoskeleton causes inhibition of NMD. The cytoskeleton thus plays a crucial role in NMD. Interestingly, disruption of actin filaments results in both inhibition of NMD and activation of premature termination codon (PTC) readthrough, while disruption of microtubules causes only NMD inhibition. Activation of PTC readthrough occurs concomitantly with the appearance of cytoplasmic foci containing UPF proteins and mRNAs with nonsense mutations but lacking the P-body marker DCP1a. These findings demonstrate that in human cells, PTC readthrough occurs in novel ‘readthrough bodies’ and requires the presence of UPF proteins.

KEY WORDS: Readthrough body, Nonsense-mediated mRNA decay, UPF protein, Cytoskeleton, P-body

INTRODUCTION

The cell cytoplasm notably contains a set of proteins forming the cytoskeleton. The cytoskeleton has three main components: (1) actin filaments consisting of actin subunits and actin-binding proteins, (2) microtubules assembled from tubulin units and microtubule-associated proteins, and (3) intermediate filaments (Fletcher and Mullins, 2010). Each element of the cytoskeleton plays a specific role. RNA transport has been mainly associated with actin filaments and microtubules, largely because the intermediate filaments are less dynamic and unable to self-organize (Aylett et al., 2011).


No association between the cytoskeleton and mRNAs harboring a premature termination codon (PTC) has yet been shown, but PTC-containing messenger ribonucleoprotein particles (PTC-mRNPs) are generated in the nucleus and exported to the cytoplasm. There, they are degraded by a surveillance mechanism called nonsense-mediated mRNA decay (NMD) (Fatscher et al., 2015; Hug et al., 2016; Karousis et al., 2016; Kervestin and Jacobson, 2012; Lejeune, 2017; Mühlemann and Lykke-Andersen, 2010; Popp and Maquat, 2014; Rebbapragada and Lykke-Andersen, 2009). In mammalian cells, several sets of factors are involved in NMD: UPF proteins [UPF1, UPF2, UPF3 (also called UPF3a) and UPF3X (also called UPF3b)], SMG proteins (SMG1, SMG5, SMG6, SMG7, SMG8 and SMG9), and components of the exon junction complex (EJC) (Chang et al., 2007; Yamashita et al., 2009). NMD not only targets mRNAs that have acquired a PTC by mutation but also regulates the expression pathways of certain ‘natural NMD substrate’ genes when a PTC arises after specific splicing events or under specific cellular conditions such as amino acid starvation or deprivation (He et al., 2003; Lelivelt and Culbertson, 1999; Mendell et al., 2004; Rehwinkel et al., 2005; Viegas et al., 2007). NMD is a cytoplasmic mechanism occurring soon after PTC-mRNP export from the nucleus (Singh et al., 2007; Treck et al., 2013). PTC-mRNPs transit through P-bodies before undergoing NMD (Durand et al., 2007). This transport might be facilitated by the cytoskeleton, although this has not yet been demonstrated. P-bodies are not organelles per se, as they are not limited by a membrane and look more like aggregates of degradative enzymes and RNAs (Cougot et al., 2004; Ingelfinger et al., 2002; Sheth and Parker, 2003; van Dijk et al., 2002). The function of P-bodies in mammalian cells remains unclear. It has been proposed that P-bodies might store enzymes capable of degrading some RNAs or be sites of RNA decay, as shown in yeast (Aizer et al., 2014; Sheth and Parker, 2003).

Although NMD can reduce the level of a PTC-mRNA by over 95% (as compared to the level of the corresponding wild-type mRNA), the efficiency of NMD depends on the target (Kuzmiak and Maquat, 2006). A proportion of each PTC-mRNA, depending on its sensitivity to NMD, thus remains available either for degradation (without translation) via the general mRNA decay pathway (You et al., 2007) or for translation into truncated proteins (Anczuków et al., 2008; Dorard et al., 2011). In the presence of various agents (e.g. aminoglycosides), PTC-mRNAs can even be translated to full-length proteins via a PTC-readthrough mechanism. Compounds facilitating PTC readthrough essentially ‘force’ the translational machinery to introduce an amino acid at the PTC position. PTC readthrough can be concomitant with NMD inhibition (Correa-Cerro et al., 2005; Gonzalez-Hilarion et al., 2012) or not (Welch et al., 2007). PTC readthrough remains largely uncharacterized, notably as regards the molecular events favoring complete translation of the open reading frame (ORF), thanks to

¹Univ. Lille, UMR8161 – M3T – Mechanisms of Tumorigenesis and Target Therapies, 59000 Lille, France. ²CNRS, UMR 8161, 59000 Lille, France. ³Institut Pasteur de Lille, 59000 Lille, France. ⁴Cellular Microbiology and Physics of Infection group – Center for Infection and Immunity of Lille, Univ. Lille, 59019 Lille, France. ⁵CNRS, UMR8204, 59019 Lille, France. ⁶Inserm, U1019, 59019 Lille, France. ⁷CHU de Lille, 59000 Lille, France. ⁸Takara Bio Europe, 78100 St-Germain-en-Laye, France. ⁹Department of Otolaryngology-Head and Neck Surgery, Eli and Edythe Broad Center for Regenerative Medicine and Stem Cell Research, Helen Diller Family Comprehensive Cancer Center, Institute for Human Genetics, Cardiovascular Research Institute, University of California, San Francisco, San Francisco, CA 94143, USA. ¹⁰Department of Pediatrics, University of Vermont College of Medicine, Burlington, VT 05405, USA. [†]Present address: Shanghai General Hospital, School of Medicine, Shanghai Jiaotong University, Shanghai 200240, China. [§]These authors equally contributed to this work

[§]Deceased

[¶]Author for correspondence (fabrice.lejeune@inserm.fr)

 J.J., 0000-0003-2065-029X; F.L., 0000-0002-5132-3585

incorporation of a given tRNA, over recruitment of release factors to the ribosome A site. The work described here offers new insights into the mechanism of NMD. The results demonstrate that NMD requires the cytoskeleton and provide evidence that nonsense codon readthrough occurs in a specific cellular environment distinct from that of normal translation. They also show that UPF protein NMD factors are required for readthrough in human cells, in contrast to what has been found in other species, such as yeast (Harger and Dinman, 2004; Salas-Marco and Bedwell, 2005; Wang et al., 2001).

RESULTS

Role of the cytoskeleton in NMD

To demonstrate a possible link between the cytoskeleton and NMD, cytoskeleton-destabilizing reagents were used to disrupt the cytoskeleton prior to assessing the efficiency of NMD: cytochalasin D was used to prevent polymerization of actin filaments, and colchicine to inhibit that of microtubules. Cytoskeleton-stabilizing reagents (promoting polymerization or preventing depolymerization) were also tested: jasplakinolide (JPK) (for actin filaments) and Taxotere (for microtubules). Cells derived from cystic fibrosis (CF) patients and harboring a nonsense mutation in the CF transmembrane conductance regulator (*CFTR*) gene were incubated for 48 h in the presence of each drug. The CF cell lines used were 6CFSMEo- and IB3, characterized by the F508del mutation (a deletion of three nucleotides encoding the phenylalanine residue at

position 508) on one *CFTR* allele and, respectively, a mutation at codon 2 (Q2X) or 1282 (W1282X, where X represents a stop codon) on the other allele, which are mutations that have been shown to act as PTCs (Cozens et al., 1992; da Paula et al., 2005; Gonzalez-Hilarion et al., 2012). Previous studies have demonstrated, at both the RNA and protein levels, very low to no *CFTR* expression in these cell lines (da Paula et al., 2005; Farinha et al., 2004; Gonzalez-Hilarion et al., 2012; Tucker et al., 2012). Cytoskeletal disruption was assessed by immunostaining of the cytoskeletal structure (Fig. 1 and data not shown for IB3 cells). In both cell lines, the agents used were found to modify actin filaments or microtubule structure (according to the target of the agent) as compared to DMSO-treated control cells. The immunostaining patterns obtained were in keeping with the mode of action of each tested drug. Under physiological conditions, actin was detected primarily in the cytoplasm. Polymerization-blocking cytochalasin D caused it to aggregate in the cytoplasm, whereas treatment with JPK stabilized actin at the cell membrane (Fig. 1A and data not shown for IB3 cells). In DMSO-treated cells, tubulin immunostaining revealed the presence of tubulin in cytoplasmic fibers (Fig. 1B and data not shown for IB3 cells). Upon colchicine treatment, the tubulin fibers were lost, whereas Taxotere treatment stabilized tubulin fiber structure by inhibiting microtubule depolymerization.

After a 48 h exposure to cytochalasin D, JPK, colchicine or Taxotere, the amount of endogenous *CFTR* mRNA was more than twice as high as in cells incubated with DMSO alone (Fig. 2A). Interestingly, the tested cytoskeleton disruptors inhibited NMD more

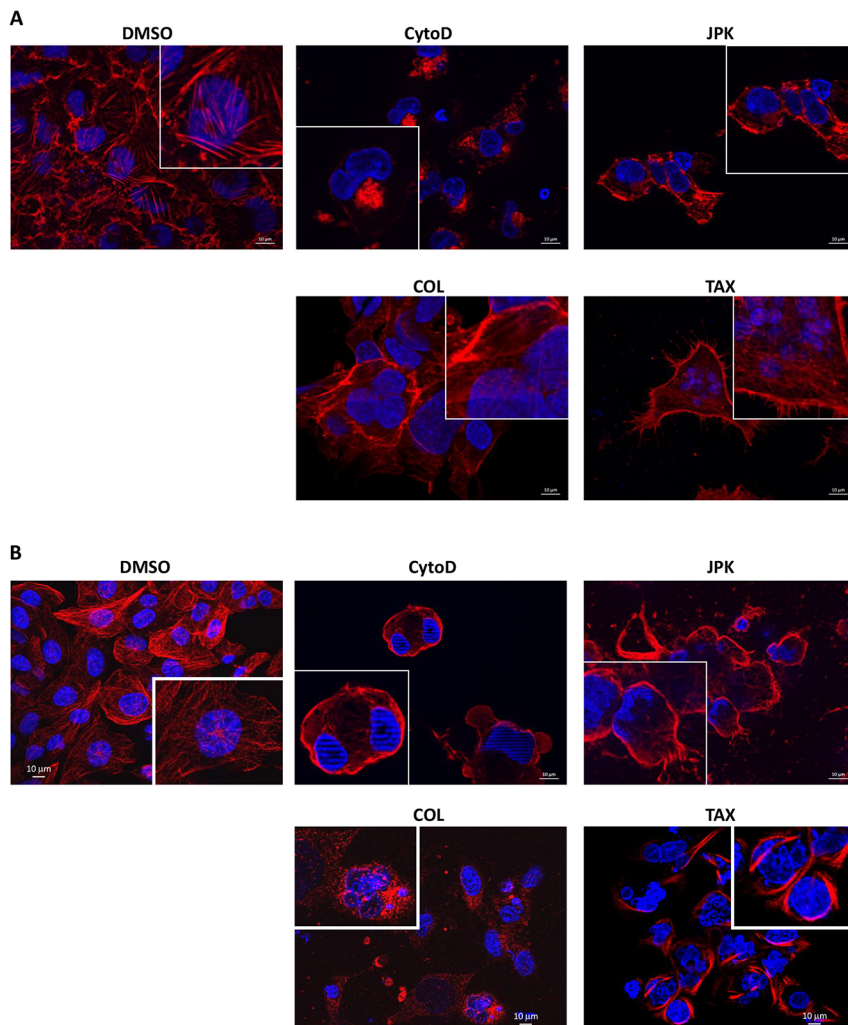


Fig. 1. Cellular distribution of the cytoskeleton under cytoskeleton inhibitor treatment. 6CFSMEo- cells were incubated with DMSO, cytochalasin D (CytoD), JPK, colchicine (COL) or Taxotere (TAX). After 48 h, the cells were fixed and permeabilized, and incubated with phalloidin to stain actin (A) or with anti-tubulin antibody followed by an Alexa Fluor 594-conjugated secondary antibody (red) for tubulin staining (B). Finally, their nuclei were visualized in blue with Hoechst 33342 stain. These results are representative of two independent experiments.

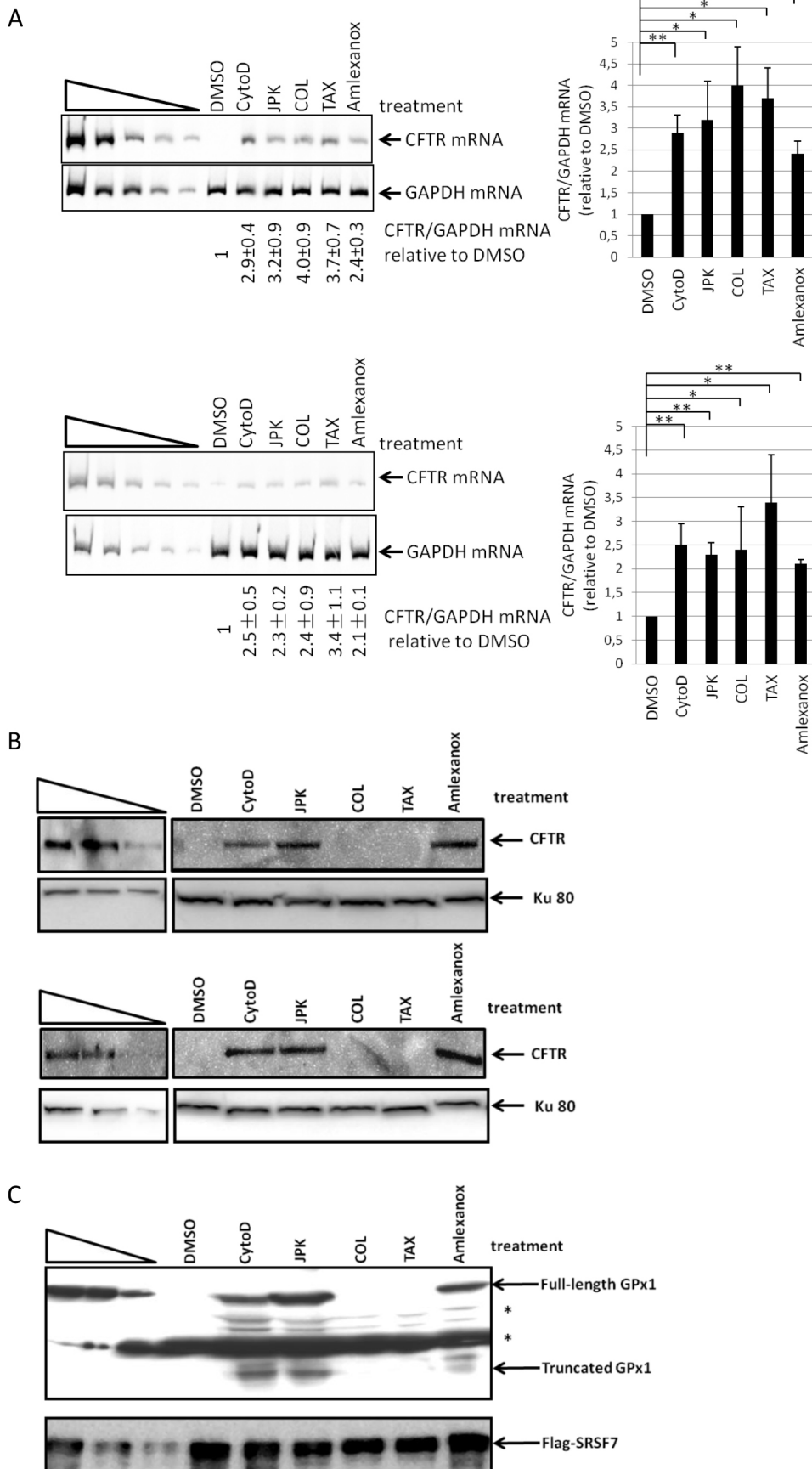


Fig. 2. Cytoskeleton disruptors influence NMD or readthrough. (A) Cytoskeleton disruptors inhibit NMD. 6CFSMEo- cells (above) and IB3 cells (below) were incubated with DMSO (negative control), cytochalasin D (CytoD), JPK, colchicine (COL), Taxotere (TAX) or amlexanox (positive control) for 48 h. The level of *CFTR* mRNA was measured by qRT-PCR and normalized to the level of *GAPDH* mRNA. The five leftmost lanes represent two-fold serial dilutions of RNA from Calu-3 cells overexpressing *CFTR* mRNA. A histogram representation of the results is presented to the right of each gel (mean±s.d.; $n=3$). (B) Actin inhibitors activate PTC readthrough of nonsense-mutation-containing *CFTR* mRNA. 6CFSMEo- cells (above) or IB3 cells (below) were incubated with DMSO, CytoD, JPK, COL, TAX or amlexanox for 48 h before analysis of protein content by western blotting. The Ku80 protein was detected as a loading control. The three leftmost lanes represent two-fold serial dilutions of protein extract from Calu3 cells. (C) Actin inhibitors promote PTC readthrough on PTC-containing mRNA introduced by transfection. 6CFSMEo- cells were transfected with an expression vector encoding YFP-tagged GPx1 46 Ter or Flag-tagged SRSF7 as a reference plasmid. The transfected cells were incubated with DMSO, CytoD, JPK, COL, TAX or amlexanox for 48 h before analysis of protein content by western blotting. Flag-tagged SRSF7 protein was used as the loading control. The three leftmost lanes represent two-fold serial dilutions of protein extract from 6CFSMEo- cells transfected with an expression vector encoding GPx1 Norm (wild type). * indicates non-specific protein species. These results are representative of three independent experiments.

effectively than amlexanox, a previously reported NMD inhibitor (Gonzalez-Hilarion et al., 2012). To rule out an indirect transcriptional effect, the level of *CFTR* pre-mRNA was measured in both cell lines. No significant variations were detected in the *CFTR* pre-mRNA level relative to the level of *GAPDH* mRNA (Fig. S1A). The effects of all cytoskeleton disruptors on the level of wild-type *CFTR* mRNA were also assessed in 16HBE14o- cells, which harbor no PTC in the *CFTR* gene (Cozens et al., 1994) (Fig. S1B). None of the treatments was found to influence the level of wild-type *CFTR*. This supports the idea that an intact cytoskeleton is required for NMD (Fig. 2A).

To make sure the above measurements of NMD were performed on viable cells, cell viability was assessed via propidium iodide staining, and the apoptosis rate was assessed by measuring Annexin V staining on cells exposed for 48 h to each of the cytoskeleton disruptors used. None of the four treatments was found to affect the viability of IB3 or 6CFSMEo- cells (Fig. S1C) or to increase their apoptosis (Fig. S1D). Thus, the NMD inhibition observed in Fig. 2A is consistent with the view that it is caused by cytoskeletal disruption and did not reflect a cytotoxic or apoptotic response to exposure to a tested drug (Fig. S1C,D).

To see whether the tested cytoskeleton disruptors inhibit only the NMD of nonsense-mutation-containing substrates or also that of 'natural NMD substrates' (Mendell et al., 2004; Sureau et al., 2001; Viegas et al., 2007), their effect was tested on three natural NMD substrates (Fig. S1E). None of the four cytoskeleton disruptors had any significant effect on levels of the chosen natural NMD substrate mRNAs. Inhibition of NMD without any effect on the regulation of natural NMD substrate mRNA levels has likewise been reported for the NMD inhibitor amlexanox (Gonzalez-Hilarion et al., 2012).

To rule out the possibility that the NMD inhibition observed with cytoskeleton inhibitors might result indirectly from inhibition of translation, 6CFSMEo- cells were incubated as described above (Fig. 2A), except that a modified amino acid was added to the medium in order to assay the levels of newly synthesized protein. In contrast to the response observed with cycloheximide (a translation inhibitor), translation proved to be unaffected by treatment with any tested drug (Fig. S1F). These results indicate that the NMD inhibition observed after treatment with cytochalasin D, JPK, colchicine or Taxotere was not an indirect effect due to altered translation.

Cytochalasin D and JPK promote PTC readthrough

Protein synthesis from PTC-mRNAs was also studied in the presence of cytoskeletal disruption, as NMD inhibitors such as G418 and amlexanox have been found to promote PTC readthrough (Correa-Cerro et al., 2005; Gonzalez-Hilarion et al., 2012). IB3 and 6CFSMEo- cells were incubated with one of the four cytoskeleton-disrupting agents or with amlexanox (as a positive control) before performing CFTR protein analysis (Fig. 2B). Full-length CFTR protein was detected in cells treated with amlexanox (as reported in Gonzalez-Hilarion et al., 2012), cytochalasin D or JPK. No full-length CFTR protein was detected after colchicine or Taxotere treatment. These findings indicate that disruption of actin filaments promotes readthrough on PTC-containing *CFTR* mRNAs, while disruption of microtubules does not. To get some idea of how general the differential effects of actin and tubulin disruption on readthrough might be, 6CFSMEo- cells were transfected with an expression construct encoding an YFP-tagged version of the glutathione peroxidase (GPx) 1 protein from mRNA that was either wild-type or carrying a PTC at codon 46 (46Ter-GPx1 mRNA) (Fig. 2C) and analyzed as above. Consistent with the observations depicted in Fig. 2B, PTC readthrough was observed on GPx1 Ter mRNA in the presence of amlexanox, cytochalasin D or JPK, but not upon treatment with colchicine or

Taxotere. As well as the full-length GPX1 protein, the truncated GPX1 protein was also detected in the presence of cytochalasin D, JPK and amlexanox. Our findings suggest that these three drugs at least facilitate translation of the GPx1 Ter mRNA. Overall, they indicate that PTC readthrough is promoted when actin filament formation is disrupted, but not upon microtubule disruption (Fig. 2B,C). Since canonical translation is not affected by treatment with cytoskeleton-disrupting agents (Fig. S1F), these results suggest that the translation occurring during readthrough is distinct from the translation occurring during canonical translation. These observations imply that PTC readthrough may require a specific intracellular localization.

When actin filaments are disrupted, UPF1 and UPF3X localize to cytoplasmic foci that are distinct from P-bodies

Previous studies have shown that inhibition of NMD can cause changes in the cellular distribution of NMD factors and substrates (Durand et al., 2007). To address this question and assess whether disrupting the cytoskeleton causes intracellular redistribution of NMD factors and substrates, 6CFSMEo- cells were transfected with an expression vector encoding an YFP-UPF1 or YFP-UPF3X protein (human proteins) (Fig. S2) and treated 1 day later with each of the four cytoskeleton-disrupting agents. The DMSO control showed a homogeneous cytoplasmic distribution of UPF1, consistent with previous findings (Durand et al., 2007; Lykke-Andersen et al., 2000; Mendell et al., 2002; Serin et al., 2001; Unterholzner and Izaurralde, 2004). After treatment with cytochalasin D, JPK, colchicine, or Taxotere, YFP-UPF1 was found to accumulate in cytoplasmic granules that appeared not to show a concentration of actin or tubulin (Fig. 1; Fig. S2A,B). UPF3X localization (mainly nuclear under physiological conditions) was altered only by JPK treatment: the protein accumulated in a subset of cytoplasmic granules that likewise did not show a concentration of actin or tubulin (Fig. S2C,D).

To test the possible involvement of the cytoskeleton in transporting PTC-mRNPs, physical interactions between NMD factors and cytoskeletal proteins were assessed in 6CFSMEo- cells under physiological conditions and under cytoskeleton disruption (Fig. 3A). In the presence of DMSO alone, UPF1, UPF2 and UPF3X were found to co-immunoprecipitate with actin or tubulin, indicating an interaction between the cytoskeleton and NMD proteins. To test whether RNAs were required for this interaction, the immunoprecipitation was repeated in the presence of RNase (Fig. 3B). In the absence of RNA, the interaction between the cytoskeletal and UPF proteins was lost. When actin or tubulin was immunoprecipitated after treatment with cytoskeleton disruptors, the UPF proteins failed to co-immunoprecipitate with the cytoskeleton (Fig. 3). Loss of the interaction between cytoskeleton and NMD factors upon cytoskeleton disruption is consistent with the observed failure of the UPF proteins to colocalize with actin or tubulin (Fig. S2).

We next assessed whether the cytoplasmic foci showing an accumulation of UPF1 and UPF3X under cytoskeleton disruption were P-bodies. To address this, the cellular localization of UPF1 and UPF3X was compared with that of the P-body marker DCP1a (Cougot et al., 2004) (Fig. 4; Fig. S3). Following colchicine or Taxotere treatment, colocalization of UPF1 foci and DCP1a foci exceeded 80%, indicating that UPF1 concentrates in P-bodies under these conditions. After cytochalasin D or JPK treatment, UPF1 foci and DCP1a foci showed only ~10% colocalization. This indicates that under these conditions, UPF1 concentrates in cytoplasmic foci that are distinct from P-bodies. Similar results were obtained when the stained protein was endogenous UPF1, rather than a tagged version produced in transfected cells (Fig. S4). These results suggest that when actin filaments are compromised, a fraction of the UPF1 is

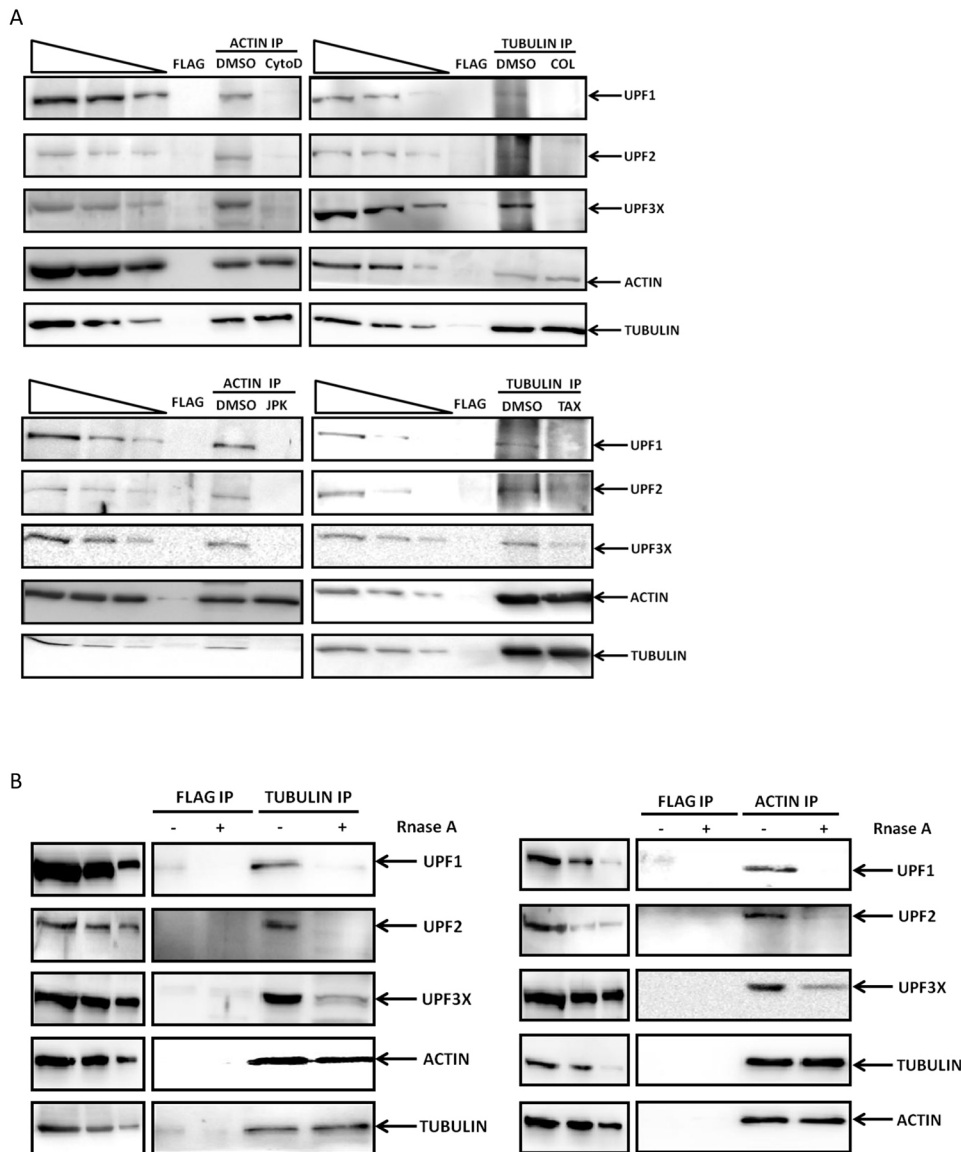


Fig. 3. Cytoskeleton inhibitors interfere with the interaction between NMD factors and the cytoskeleton. (A) 6CFSMEo- cells were incubated with DMSO, cytochalasin D (CytoD), JPK, colchicine (COL) or Taxotere (TAX) for 48 h before protein extraction and immunoprecipitation (IP) with anti-actin, anti-tubulin, or, as a negative control, anti-Flag antibodies. Western blotting was performed to detect the presence of UPF1, UPF2, UPF3X, tubulin and actin. (B) The interaction between NMD factors and the cytoskeleton requires RNA. Protein-containing lysate of 6CFSMEo- cells was incubated with 10 mg/ml BSA or RNase A before immunoprecipitation with anti-actin, anti-tubulin, or anti-flag antibody (negative control). The level of UPF1, UPF2, UPF3X, tubulin, or actin protein was analyzed by western blotting. The three leftmost lanes of each western blot represent two-fold serial dilutions of protein extract from 6CFSMEo-cells. These results are representative of two independent experiments.

sequestered in cytoplasmic foci that are not P-bodies, and that actin filaments may be required for UPF1 exit from these new cytoplasmic foci. The localization pattern of UPF3X upon JPK treatment was similar to that of UPF1; UPF3X was found to concentrate at foci showing only ~10% colocalization with P-bodies (Fig. S3).

The specific cellular distribution of UPF proteins observed under cytoskeleton disruption raises the possibility that cytoskeleton disruption might also affect the cellular distribution of PTC-mRNAs. To test this possibility, the cellular localization of GPx1 Ter PTC-mRNAs (Moriarty et al., 1998) was analyzed after treatment with cytochalasin D, JPK, colchicine or Taxotere (Fig 5; Fig. S5). The localization patterns observed were the same as for the UPF1 and UPF3X proteins (Fig 4; Fig. S3). In contrast, the wild-type version of GPx1 mRNA (GPx1 Norm) did not localize to cytoplasmic foci after disruption of cytoskeleton (Fig. S6). The redistribution observed with GPx1 Ter PTC-mRNA thus appears specific to PTC-mRNAs.

Consistent with the above observations, GPx1 Ter mRNA colocalization with DCP1a was high after colchicine or Taxotere treatment, and low after cytochalasin D or JPK treatment (Fig. S7). These results indicate that NMD substrates and NMD factors are

sequestered in P-bodies when microtubules are disrupted but concentrate primarily in other, novel, cytoplasmic foci when actin filaments are disrupted.

When readthrough is activated, PTC-mRNAs predominantly localize to the novel cytoplasmic foci

The identity of the novel foci containing UPF1, UPF3X and PTC-mRNAs after actin filament disruption was investigated by comparing the cellular localization of the UPF proteins with those of various organelle markers. No colocalization was observed between UPF1 or UPF3X and the stress granule marker protein eIF3 β (Brown et al., 2011) or the autophagosome marker protein LC3B (also known as MAP1LC3B) (Tanida et al., 2008) (Figs S8, S9). This indicates that upon actin filament disruption, NMD factors and substrates concentrate in cytoplasmic foci that are distinct from P-bodies, stress granules and autophagosomes, and these foci are therefore a new category of cytoplasmic foci.

The fact that the new cytoplasmic foci were detected after cytochalasin D or JPK treatment suggests that they could be related to the readthrough process, since readthrough was also observed after cytochalasin D or JPK treatment (Figs 2B,C, 4–6; Figs S3 and

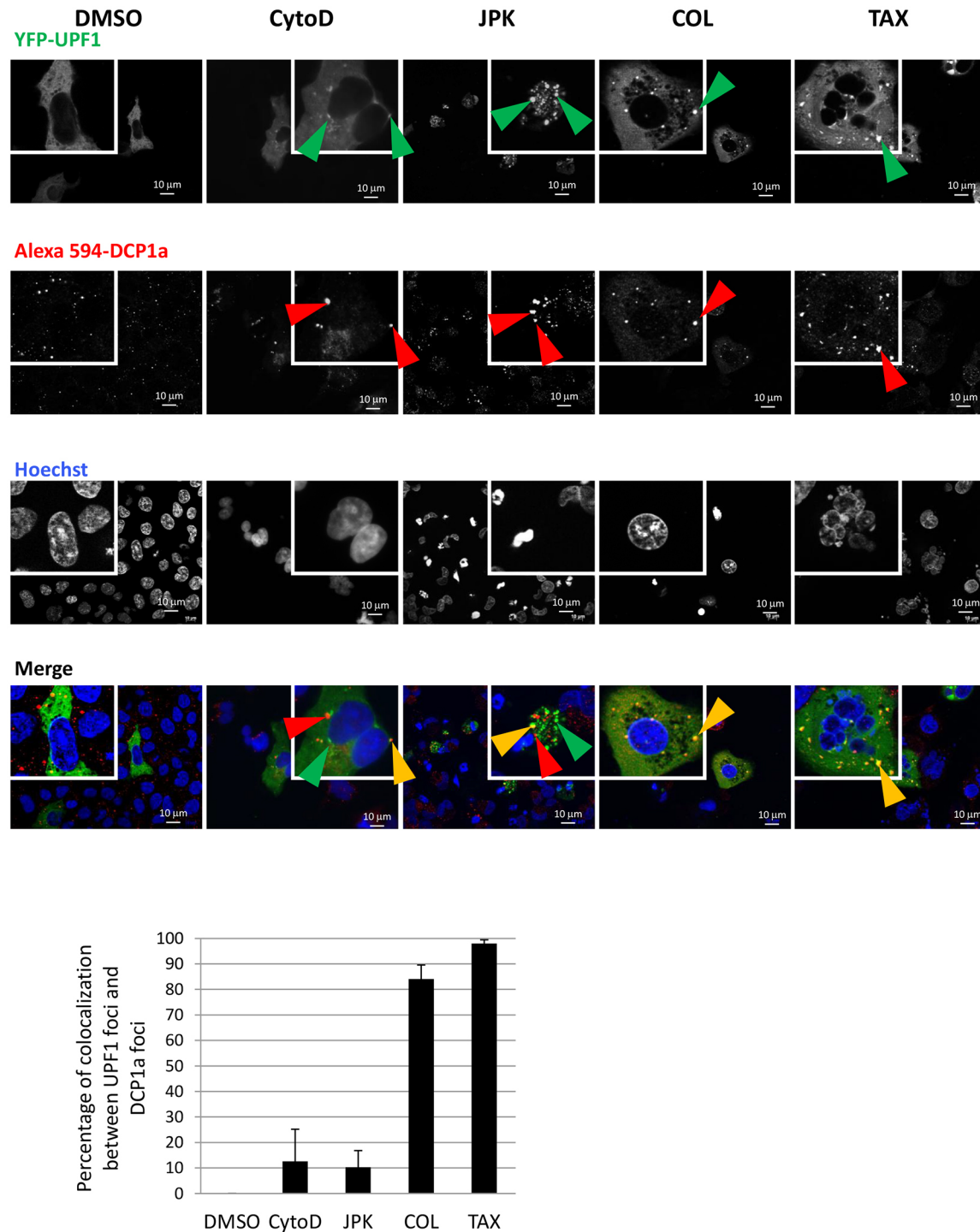


Fig. 4. In 6CFSMEo- cells, UPF1 protein is concentrated partially or totally in P-bodies after cytoskeleton inhibitor treatment. Cells were transfected with constructs expressing YFP–UPF1 and GPx1 Ter and then incubated with DMSO, cytochalasin D (CytoD), JPK, colchicine (COL) or Taxotere (TAX) for 48 h. After fixation and permeabilization, the cells were incubated first with anti-DCP1a primary antibody and then with the Alexa Fluor 594-conjugated secondary antibody (red). Finally, the nuclei were visualized in blue by Hoechst 33342 staining. Green arrowheads indicate UPF1 cytoplasmic foci; red arrowheads indicate the P-body marker DCP1a; orange arrowheads indicate colocalization of UPF1 and DCP1a. The histogram represents the percentage of colocalization between UPF1 foci and DCP1a foci. Cells (mean±s.d.; $n=10$) from three different experiments were counted for each condition.

S5–7). To confirm this hypothesis, the cellular localization of UPF1 was studied after treatment with G418, a reference readthrough-inducing molecule (Gatti, 2012; Manuvakhova et al., 2000; Shalev et al., 2013) (Fig. 6), or amlexanox (Fig. S10). When readthrough was induced with G418 or amlexanox, a limited fraction of the UPF1 was found sequestered in P-bodies, but most of it was found

sequestered in another type of cytoplasmic foci containing no DCP1a. Under G418 treatment, furthermore, PTC-mRNAs fully colocalized with UPF1-containing cytoplasmic foci. In contrast, wild-type mRNA failed to concentrate in cytoplasmic foci under G418 treatment (Fig. S11). Overall, these results suggest that upon readthrough activation, PTC-mRNPs are moderately concentrated

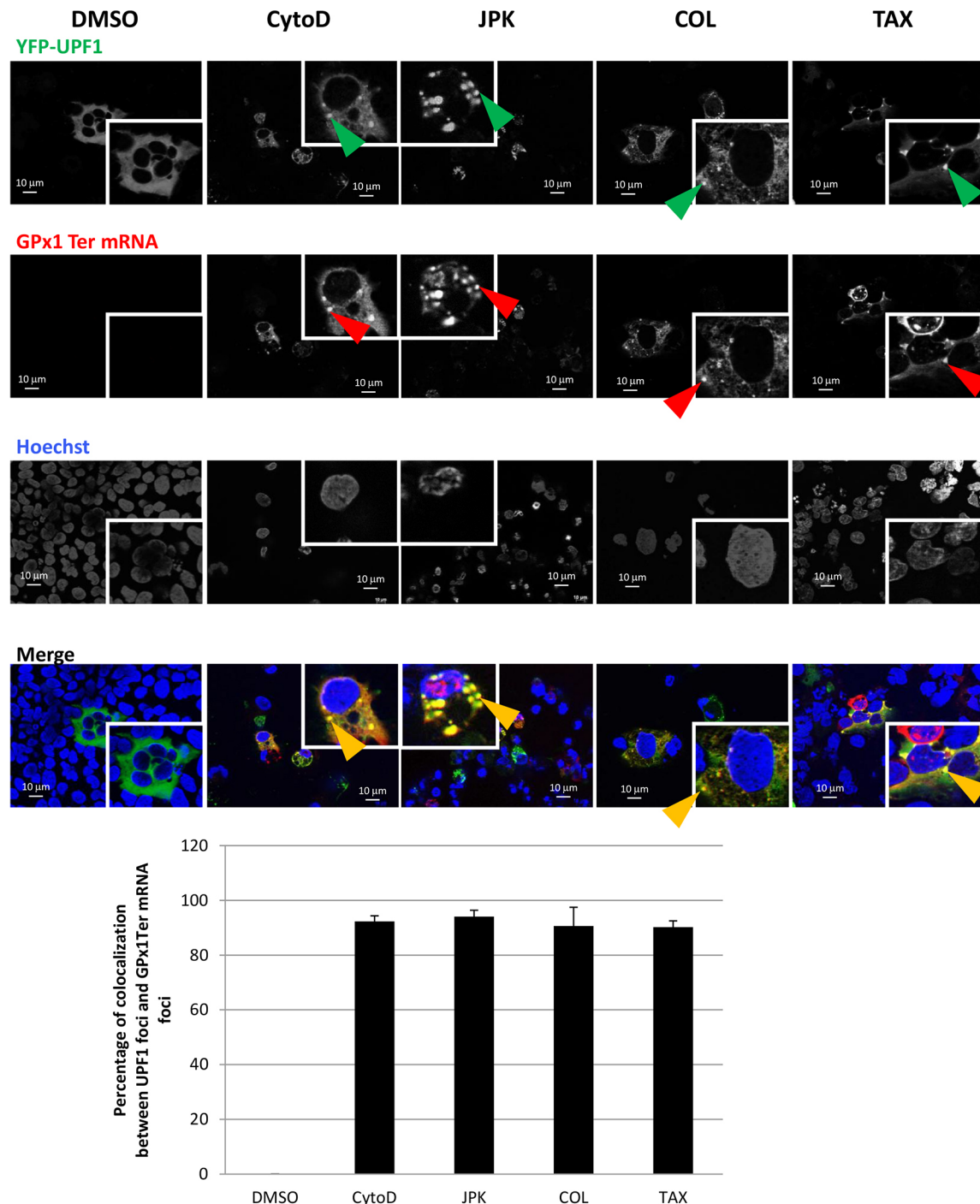


Fig. 5. In 6CFSMEo- cells, the NMD factor UPF1 colocalizes with NMD substrates under cytoskeleton disruptor treatment. 6CFSMEo- cells were transfected with constructs expressing GPx1 Ter and YFP-UPF1 and then incubated with DMSO, cytochalasin D (CytoD), JPK, colchicine (COL) or Taxotere (TAX) for 48 h. A fluorescence *in situ* hybridization (FISH) assay was performed to detect the cellular localization of GPx1 Ter mRNA. Nuclei are stained in blue with Hoechst 33342 stain. Green arrowheads indicate UPF1 cytoplasmic foci; red arrowheads indicate mRNA cytoplasmic GPx1 mRNA foci; orange arrowheads indicate colocalization of the UPF1 factor and NMD substrates. The histogram represents the percentage of colocalization between UPF1 foci and GPx1 Ter. Cells (mean \pm s.d.; $n=10$) from three different experiments were counted for each condition.

in P-bodies but are predominantly found in a new type of cytoplasmic foci.

Further evidence supporting the existence of readthrough-related foci that are distinct from P-bodies was obtained by measuring the distance between the new cytoplasmic foci and P-bodies with ImageJ software (Fig. S12A). Under colchicine or Taxotere treatment, the DCP1a and the UPF1 foci were mainly found to

overlap. Upon G418 or cytochalasin D treatment, the DCP1a foci and UPF1 foci appeared to be separated from each other, the distance between them usually being less than 2 μ m.

To study the dynamics of the new cytoplasmic foci relative to P-bodies, a fluorescence recovery after photobleaching (FRAP) assay was performed under different conditions. 6CFSMEo- cells were transfected with two expression vectors: one encoding RFP-DCP1a,

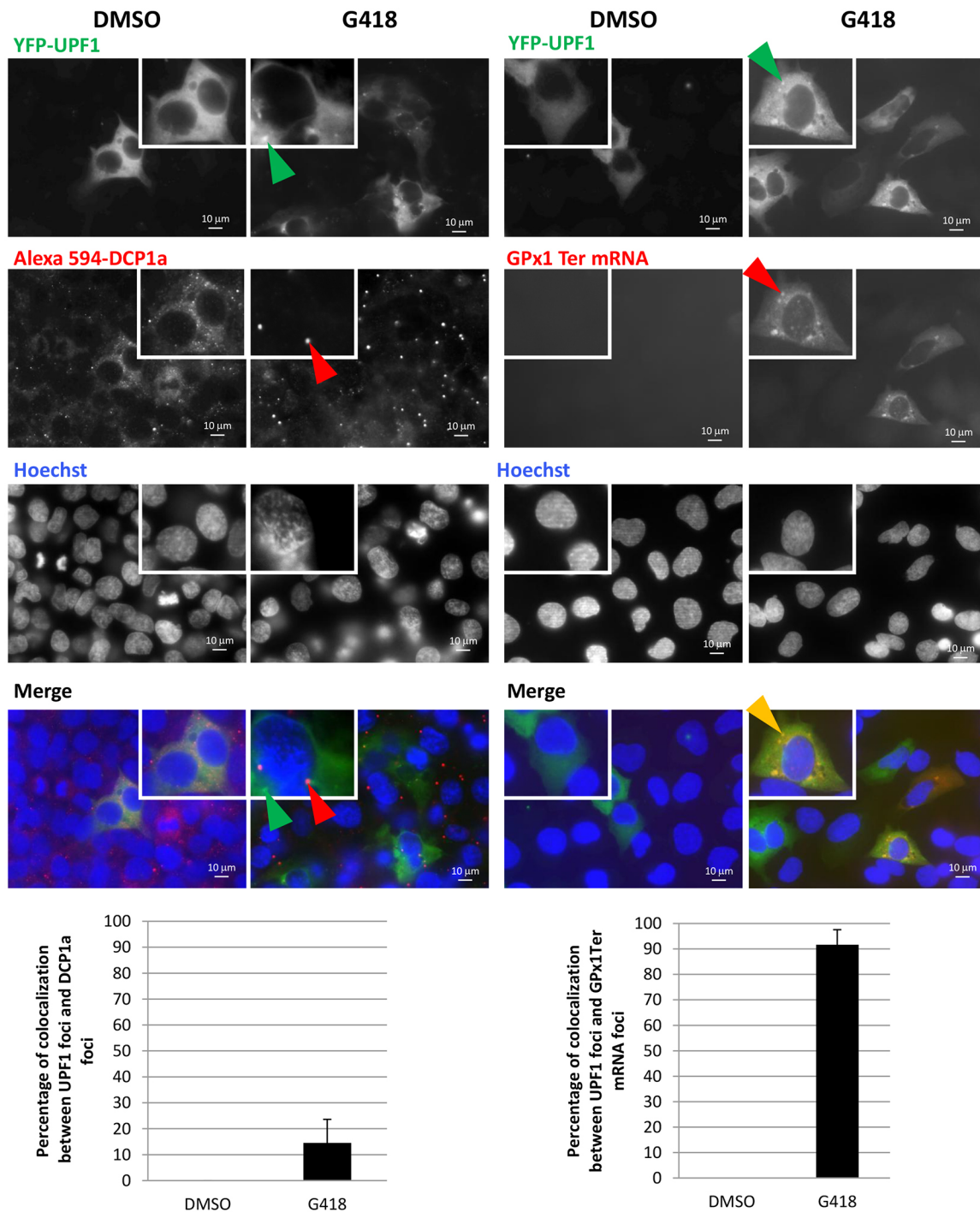


Fig. 6. G418 causes UPF1 to localize to cytoplasmic foci containing NMD substrates but not the P-body marker DCP1a. 6CFSMEo-cells were transfected with constructs expressing YFP-UPF1 or GPx1 Ter before treatment with G418 at 400 μ g/ml for 48 h. Left panel, cells were incubated sequentially with anti-DCP1a antibody and Alexa Fluor 594-conjugated secondary antibody (red). Right panel, cells were incubated with a GPx1 fluorescence *in situ* hybridization (FISH) probe. The percentage of colocalization between UPF1 and DCP1a (left) or between UPF1 and GPx1 Ter mRNA (right) is presented in histograms at the bottom of the figure. Cells (mean \pm s.d.; $n=10$) from three different experiments were counted for each condition. Nuclei were stained with Hoechst 33342 solution (blue). Green arrowheads indicate UPF1 cytoplasmic foci; red arrowheads indicate P-bodies or foci containing GPx1 mRNA; orange arrowheads indicate colocalization foci.

as a marker of P-bodies, and one encoding YFP-UPF1, so as to observe the dynamics of the new cytoplasmic foci (Fig. S12B). Upon cytochalasin D treatment, no fluorescence recovery was observed after photobleaching. This indicates that both DCP1a and UPF1 require the cytoskeleton to move, respectively, to P-bodies or to the new cytoplasmic foci. Under G418 treatment, some fluorescence was

recovered by both cytoplasmic foci, indicating that both proteins could still move. In P-bodies, the maximum recovery ($\sim 20\%$) was reached in 20 s, as previously reported (Andrei et al., 2005). A quite similar fluorescence recovery rate was observed for the new cytoplasmic foci (Fig. S12B, green curves). The two structures thus show similar dynamics.

To rule out the possibility that the new cytoplasmic foci might be an artifact related to use of a drug, an siRNA against actin was designed. The use of this siRNA in 6CFSMEo- cells promoted inhibition of NMD, as shown by an increase in *CFTR* mRNA (Fig. S13A). It was also found to activate readthrough, as shown by detection of full-length *CFTR* protein (Fig. S13A). Consistent with these results, cytoplasmic foci containing *UPF1* and GPx1 Ter mRNA but not *DCP1a* were detected upon actin knockdown (Fig. S13B).

The new cytoplasmic foci are the site of readthrough in the cell

Although we were unable to detect RPL13, eIF5A or PABP protein in the new cytoplasmic foci (data not shown), likely because readthrough would occur at a much lower level than canonical translation, we hypothesized that these foci might be the place where readthrough occurs. To validate this hypothesis, we examined whether readthrough proteins might be synthesized in the new cytoplasmic bodies. For this, the GPx1 Ter gene was fused C-terminally to the sequence encoding the Neptune tag under the control of a TET-inducible promoter. The resulting construct was expressed in 6CFSMEo- cells after transient transfection, together with an expression vector encoding YFP-UPF1 and another encoding RFP-DCP1a. The transfected cells were incubated with cytochalasin D for 48 h before addition of doxycycline to the medium to promote synthesis of the C-terminally Neptune-tagged version of GPx1 Ter. It was reasoned that the appearance of Neptune fluorescence should show where PTC readthrough occurs. Pictures were taken with a confocal microscope every 2 min over a 1 h period starting about 10 min after doxycycline addition (Movie 1; Fig. 7). The results show that the Neptune signal was stronger in samples exposed to doxycycline than it was prior to doxycycline exposure. The presence of a Neptune signal in the absence of doxycycline reflects some leakage of the promoter, as previously reported (Zeng et al., 1998). Interestingly, the Neptune signal was confined to certain cytoplasmic foci, and the location of these foci was compared to that of DCP1a and UPF1. All newly detected Neptune signals were observed in cytoplasmic foci containing UPF1 but not DCP1a. This confirms that readthrough occurs in the new cytoplasmic foci. In addition, the translation observed in the new cytoplasmic foci appeared to concern only PTC-containing mRNAs, since no translation of a wild-type GPx1-Neptune-encoding mRNA was found to occur there (Movie 2). When the experiment was performed in the presence of the translation inhibitor cycloheximide, no Neptune signals were detected in the cells (Movie 3). We thus coined the term ‘readthrough bodies’ to designate the cytoplasmic foci where readthrough occurs.

UPF proteins are required for PTC readthrough

The presence of UPF1 in readthrough bodies suggests that UPF1 could play a role in readthrough. To test this possibility, 6CFSMEo-cells were transfected with a control siRNA or with an siRNA targeting endogenous UPF1 (Mendell et al., 2002). The cells were then incubated with DMSO, cytochalasin D or G418 before extracting proteins and detection of full-length *CFTR* protein by western blotting. As shown in Fig. 8A, and consistent with the results of Fig. 2B,C, the *CFTR* protein was detected in control-siRNA-treated cells upon incubation with cytochalasin D or G418, but not after incubation with DMSO (lanes 2 and 3 compared to lane 1). In UPF1-knockdown cells, the *CFTR* protein was not detected, even in the presence of cytochalasin D or G418 (lanes 7–9). Hence, UPF1 is required for nonsense mutation readthrough. To confirm the

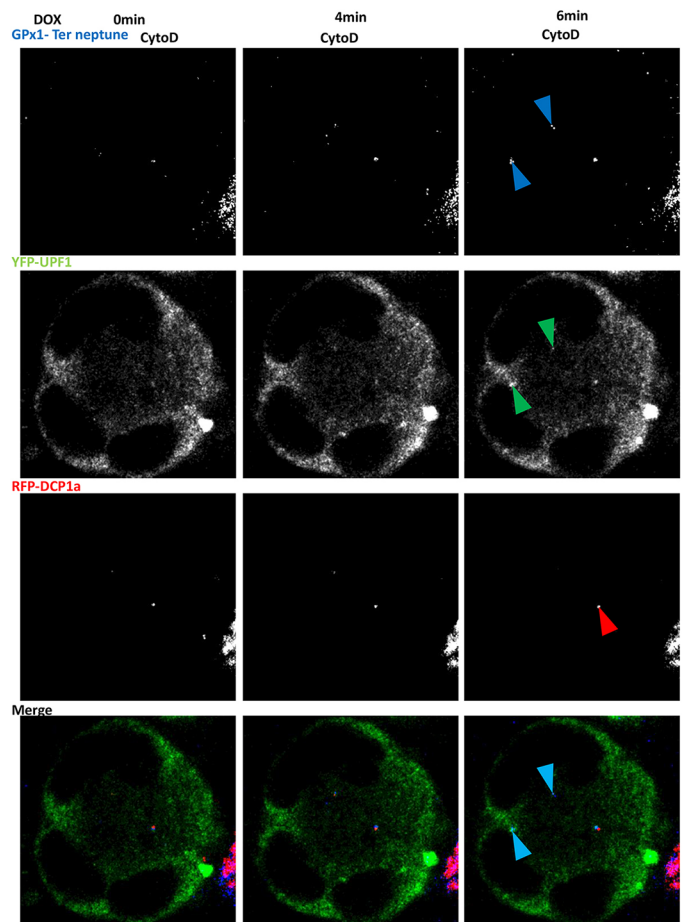


Fig. 7. Readthrough GPx1 Ter-Neptune proteins colocalize with UPF1 under cytochalasin D treatment. 6CFSMEo- cells transfected with plasmids encoding YFP-UPF1 (green), RFP-DCP1a (red), and GPx1 Ter-Neptune (blue) were treated with cytochalasin D (CytoD). After 48 h, doxycycline was added to the medium and pictures were taken every 2 min for 1 h under confocal laser scanning microscopy. Pictures taken at 0, 4 and 6 min after adding doxycycline are shown here. Blue arrowheads indicate the GPx1 protein; green arrowheads indicate the UPF1 protein; red arrowheads indicate P-bodies; cyan arrowheads indicate colocalization foci.

specificity of downregulation by the UPF1-targeting siRNA, cells were transfected with a construct expressing an siRNA-resistant isoform of the UPF1 protein. The siRNA-resistant isoform of UPF1 was found not to interfere with the production of readthrough *CFTR* under cytochalasin D or G418 treatment, as demonstrated in the presence of the control siRNA (lanes 4–6). The effect of the UPF1-targeting siRNA was inhibited in the presence of the siRNA-resistant isoform of UPF1, since full-length *CFTR* was detected in cells treated with cytochalasin D or G418 (lanes 10–12). This validates the conclusion that UPF1 is necessary for PTC readthrough.

To determine whether UPF1 is the only NMD factor required for readthrough, UPF2 or UPF3X was knocked down with siRNA and readthrough was induced with cytochalasin D or G418 (Fig. 8B,C). A significant decrease in the level of UPF2 or UPF3X protein was found to fully inhibit readthrough induced by cytochalasin D or G418. Overall, the results of Fig. 8 demonstrate that readthrough requires the UPF proteins in human cells.

Since readthrough is inhibited when UPFs are downregulated, another way to confirm that readthrough occurs in readthrough bodies is to check whether readthrough bodies persist in the presence of a

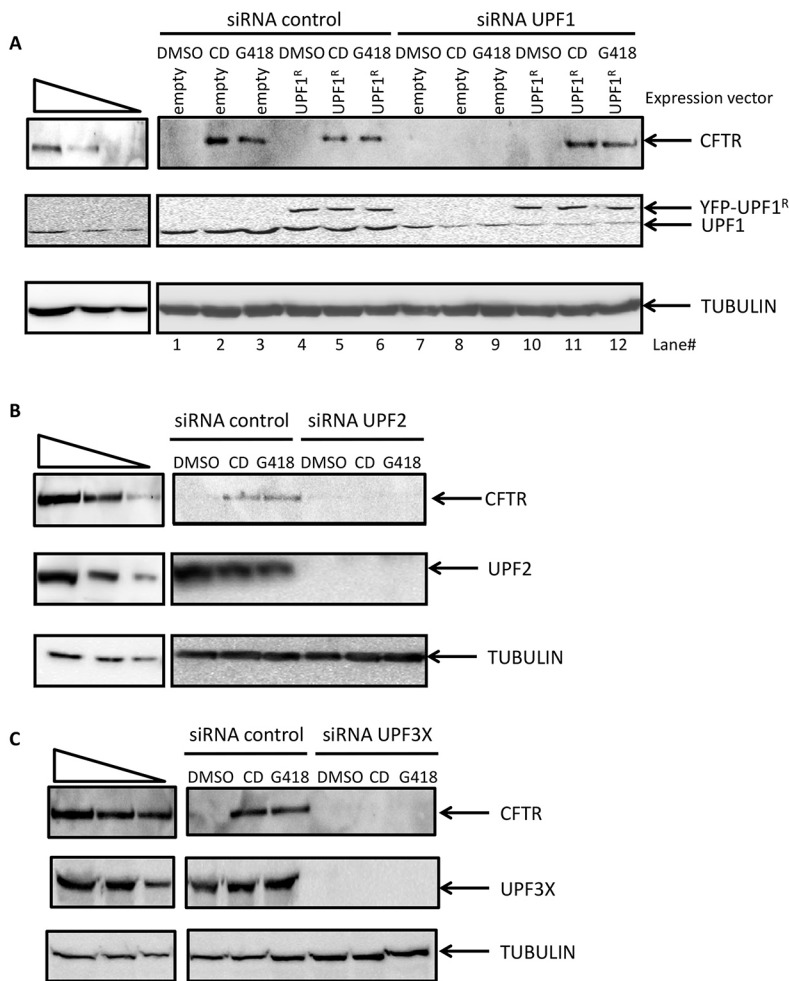


Fig. 8. Downregulation of UPF proteins inhibits PTC readthrough.

6CFSMEo- cells were transfected with (A) control or UPF1 siRNA, with or without a plasmid expressing an siRNA-resistant UPF1 isoform (UPF1^R), (B) control or UPF2 siRNA, or (C) siRNA control or UPF3X siRNA. At 24 h after transfection, the cells were incubated with DMSO, cytochalasin D (CD) or 400 µg/ml G418 for 48 h before estimation of the protein content by western blotting. Levels of CFTR, UPF1, UPF2 and tubulin (as loading control) were estimated. The three leftmost lanes represent two-fold serial dilutions of protein extract from Calu-3 cells. These results are representative of three independent experiments.

UPF-targeting siRNA in cells incubated with readthrough molecules (Fig. S13). In the presence of a control siRNA, both G418 and cytochalasin D were found to promote stabilization of the NMD substrate GPx1 Ter mRNA and its concentration in P-bodies and readthrough bodies (Fig. S13B–F). When the UPF proteins were knocked down with siRNAs (Fig. S13B,D,E), labeled GPx1 Ter mRNA became detectable in DMSO-treated cells because of the resulting NMD inhibition (see Fig. S13F for the efficiency of NMD inhibition). As previously reported (Durand et al., 2007), the GPx1 Ter signal appeared to be homogeneously distributed throughout the cytoplasm in DMSO-treated cells. In the presence of G418 or cytochalasin D, GPx1 Ter mRNA did not concentrate in P-bodies or readthrough bodies. This is consistent with the view that the UPF proteins are required to form readthrough bodies (Fig. S13D,E).

DISCUSSION

In cells, the cytoskeleton ensures transport of various cellular structures and molecules such as proteins and nucleic acids, including mRNAs (Bassell et al., 1999; Fletcher and Mullins, 2010; Lopez de Heredia and Jansen, 2004). We thus hypothesized that PTC-mRNAs might be transported by the cytoskeleton to their degradation sites in the cytoplasm. In support of this hypothesis, we demonstrate here that disrupting actin or tubulin filaments leads to inhibition of NMD (Figs 1,2A) and that the observed inhibition is not an indirect effect due to altered transcription or increased cell death (Fig. S1). In addition, we show that cytoskeleton disruptors cause stronger NMD inhibition than amlexanox, without affecting

the translation mechanism (Fig. S1F) or the regulation of natural NMD substrates (Fig. S1E). Our results thus show that cytoskeleton disruptors constitute, alongside translation inhibitors and apoptosis inducers (Jia et al., 2015; Popp and Maquat, 2015), a new family of effective NMD inhibitors.

Since translation appears unaffected by cytoskeleton inhibitors, and since we and others have previously shown that some NMD inhibitors can also activate readthrough (Correa-Cerro et al., 2005; Gonzalez-Hilarion et al., 2012), we investigated whether full-length proteins can be synthesized from PTC-mRNAs after cytoskeleton disruption (Fig. 2B,C). Interestingly, our results demonstrate readthrough in the presence of actin filament disruptors but not in the presence of microtubule disruptors, suggesting that readthrough requires microtubules and that the absence of actin filaments favors PTC readthrough.

Although we do not favor it, we cannot exclude the hypothesis that the activation of PTC readthrough and/or the inhibition of NMD by cytoskeleton disruptors might be an indirect effect. For example, NMD inhibition might be caused by failure of an essential NMD factor to be transported to P-bodies. Alternatively, the alteration of actin filaments by cytochalasin D or JPK might lead to the absence of a factor responsible for PTC recognition on PTC-mRNAs, thus causing increased PTC readthrough. In-depth analysis of the protein composition of PTC-mRNPs in cells treated with cytochalasin D or JPK should provide information supporting or ruling out these possibilities and should contribute to better understanding of the molecular role of the cytoskeleton in NMD and PTC readthrough.

We further show that P-bodies are the structures where UPF1 concentrates when the microtubules are disrupted (Fig. 4), consistent with sequestration of NMD factors in P-bodies in some cases of NMD inhibition (Durand et al., 2007). When actin filaments are disrupted, on the other hand, UPF1 and UPF3X concentrate to some extent in P-bodies, but are mostly found in another type of cytoplasmic foci that is distinct from stress granules and autophagosomes (Fig. 4; Figs S3, S4, S9). PTC-mRNAs also concentrate in P-bodies upon microtubule disruption and but are also mostly found in the new type of UPF1-containing cytoplasmic foci upon actin filament disruption (Fig. 5; Figs S5, S7). The fact that this cellular distribution pattern is not observed with wild-type mRNAs (Fig. S6) indicates that PTC-mRNPs are specifically addressed to P-bodies and to the new cytoplasmic foci.

Since the same conditions appear to favor both PTC readthrough and the appearance of the new cytoplasmic foci, we examined whether the latter might be the place where readthrough occurs. Consistent with this idea, the new cytoplasmic foci were detected when amlexanox or the reference readthrough molecule G418 was used to elicit PTC readthrough (Fig. 6; Fig. S10). In addition, newly synthesized readthrough proteins were detected in the new cytoplasmic foci and not in P-bodies. This demonstrates that readthrough occurs in the newly discovered bodies, which we have therefore named readthrough bodies (Fig. 7; Movie 1). Our results indicate that readthrough and the translation of wild-type mRNAs occur in distinct environments (Movie 2). They suggest that readthrough requires specific factors and is subject to dedicated regulation, requiring further investigation. In support of this idea, UPF1 and UPF3X are found in readthrough bodies, and downregulation of UPF1, UPF2 or UPF3X results in inhibition of readthrough (Fig. 8; Fig. S13). These results reveal a new function for UPFs: a role in PTC readthrough. This role is an additional argument in favor of separation of readthrough from translation, since downregulation of UPF proteins has no impact on translation (Isken et al., 2008) but does affect PTC readthrough. Our observation that downregulation of UPF proteins abolishes readthrough highlights an additional difference in the roles played by UPF proteins in yeast and mammals. The situation in yeast remains somewhat controversial: some studies have demonstrated increased readthrough, attributed to defective translation termination, in yeast cells lacking of one of the UPF proteins (Salas-Marco and Bedwell, 2005; Wang et al., 2001), while another has concluded that UPF proteins have no involvement in readthrough in yeast (Harger and Dinman, 2004). The present study on human cells leads to a very different conclusion: that in mammals, these proteins play a role in PTC readthrough, since downregulation of UPF1, UPF2 or UPF3X abolishes this process (Fig. 8). The mechanism of readthrough remains largely unexplored, and no specific proteins involved in this process had been previously identified in mammals. Our finding that the absence of UPF proteins impairs readthrough and not translation sheds some light on the molecular mechanism of readthrough.

Recently, readthrough of physiological stop codons has been demonstrated in the case of four genes in human cells (Loughran et al., 2014). Further studies will be necessary to determine whether UPF proteins are also required for readthrough of physiological stop codons. It will be also interesting to identify the cellular site of physiological stop codon readthrough, in order to determine whether readthrough bodies are specialized solely in PTC readthrough or whether stop codon readthrough also occurs there.

The relationship between P-bodies and readthrough bodies needs to be further studied. One question is: do readthrough bodies derive from P-bodies through addition/removal of certain factors, or are

they pre-existing entities that exchange certain mRNPs with P-bodies? The latter hypothesis seems more plausible, since P-bodies are detected in the presence and absence of the cytoskeleton and thus appear to be independently stable. In addition, both structures are found in close vicinity to each other (Fig. S12). A clear demonstration of transfer will require identifying a specific and stable marker of readthrough bodies, just as the stability of P-bodies under physiological conditions can be demonstrated by monitoring the cellular localization of a permanent P-body component such as DCP1a.

Finally, our results show that cytoskeleton disruptors can inhibit NMD and/or activate PTC readthrough. Some molecules, such as Taxotere and colchicine, are used to treat pathologies (cancer and gout, respectively, in the case of these agents). Given the effects of these molecules on NMD and readthrough, it would be interesting to investigate their use in, for example, treatment of cancers related to the presence of a nonsense mutation in a tumor suppressor gene. Such applications would constitute a new type of targeted therapy for cancers.

MATERIALS AND METHODS

Chemicals

Cytochalasin D and jasplakinolide (JPK) were obtained from Enzo Life Sciences. Colchicine was purchased from Sigma-Aldrich (Lyon, France) and Taxotere was obtained from Selleck Chemicals. Amlexanox was purchased from Sequoia Research. Each molecule was dissolved in DMSO except G418 (GIBCO), which was dissolved in water. Cytochalasin D, JPK and Taxotere were each used at 1 μ M, colchicine at 10 μ M, amlexanox at 25 μ M, and G418 at 400 μ g/ml.

Cell culture

IB3 cells (ATCC-CRL-2777) harboring a nonsense mutation in exon 20 of the *CFTR* gene were grown in LHC-8 (without gentamicin) supplemented with 10% fetal bovine serum (FBS) and Zell shield (Minerva Biolabs, Berlin, Germany) to prevent mycoplasma contamination. 6CFSMEo- cells (Cozens et al., 1992) harboring a nonsense mutation in exon 1 of the *CFTR* gene were grown in α -MEM supplemented with 10% FBS, 1 mM L-glutamine and Zell shield. Calu-3 cells (ATCC-HTB-55) overexpressing CFTR protein were grown on RPMI with 10% FBS and Zell shield. Cells were incubated with the specified molecule or with DMSO as a negative control for 48 h at 37°C under 5% CO₂.

qRT-PCR analysis

Quantitative RT-PCR (qRT-PCR) was performed as described previously (Gonzalez-Hilarion et al., 2012). The primer sequences used in this study were for: *GAPDH* (sense, 5'-CATTGACCTCAACTACATGG-3'; antisense 5'-GCCATGCCAGTGAGCTTCC-3'), *CFTR* (sense, 5'-GGCCAGAGG-GTGGGCCTCT-3'; antisense, 5'-AGGAACTGTTCTATCACAG-3'), *CFTR* pre-mRNA (sense, 5'-TTGATGCCTAGAGGGCAGAT-3'; antisense, 5'-TGTCAAAGGGATTGGGAGGG-3'), *SC35* (also known as *SRSF2*) (sense, 5'-CCTCTTAAGAAAATGCTGCGGTCTC-3'; antisense, 5'-ATCAGCCAAATCAGTAAAATCTGC-3'), *NAT9* (sense, 5'-ATTG-TGCTGGATGCCGAGA-3'; antisense, 5'-ACCTAGCGTGGTCACTC-CGTA-3'), and *TBL2* (sense, 5'-GCAGTCATTTACCACATGC-3'; antisense, 5'-TATTGTTTCTGCTTCTTGAT-3').

Western blot analysis

Proteins were extracted in the following lysis buffer: 50 mM Tris-HCl pH 7.0, 20 mM EDTA and 5% SDS. The *CFTR* protein was analyzed by separating on a 3–8% precast NuPAGE gel (Life technologies) and transfer to nitrocellulose membrane by i-blot transfer (Life technologies). Migration of all the other proteins was carried out in a 10% SDS-PAGE gel. After migration, the proteins were transferred to a nitrocellulose membrane and incubated with primary antibodies overnight at 4°C before incubation with a secondary antibody [111-035-003 (rabbit) or 115-035-003 (mouse), Jackson

Immuno Research, West Grove, PA] at 4°C for 2 h. Finally, the proteins were observed with SuperSignal West Femto Maximum Sensitivity Substrate (Pierce-Biotechnology, Rockford, IL, USA). The primary antibodies used were: rabbit anti-UPF1 antibody at 1:5000 (ab86057, Abcam, Paris, France), rabbit anti-UPF2 antibody at 1:5000 [antibody raised against the following synthetic peptide: H₂N-MPAERKKPASMEEKDC-CONH₂ (Eurogentec, Angers, France)], rabbit anti-UPF3X antibody at 1:5000 (ARP40998_T100, Aviva Systems Biology, San Diego, CA), rabbit or mouse anti-actin antibody at 1:1000 (ab8227/ab3280, Abcam), rabbit anti-tubulin antibody at 1:1000 (PM054, Epitomics, Burlingame, CA), anti-human CFTR C-terminus monoclonal antibody (clone 24-1) at 1:1000 (R&D Systems, Abingdon, UK), rabbit anti-GFP antibody at 1:1000 (G1544, Sigma-Aldrich, Lyon, France), rabbit anti-flag at 1:1000 (F1804, Sigma-Aldrich) or rabbit anti-Ku80 (also known as XRCC5) antibody at 1:1000 (Epitomics).

Immunocytochemistry

6CFSMEO- cells were incubated on 12-mm coated slides and transfected with 250 ng plasmids expressing YFP-UPF1 or YFP-UPF3X and pCMV-GPx1 Ter. Coating was performed with a solution made of LHC-8 medium containing 0.1 mg/ml BSA, 0.03 mg/ml collagen I, rat tail (Gibco) and 0.01 mg/ml human fibronectin (Sigma-Aldrich). At 24 h after transfection, the cells were treated with 1 μM cytochalasin D, 1 μM JPK, 10 μM colchicine, 1 μM Taxotere or DMSO for 48 h. They were then fixed with 10% formalin for 10 min at room temperature, washed three times with Dulbecco's PBS, and permeabilized with 70% ethanol for 1 h at 4°C. Fixed cells were incubated with primary antibodies [anti-actin (Abcam, ab3280, dilution 1:1000), anti-tubulin (Epitomics, PM054, dilution 1:1000), anti-DCP1a (Sigma-Aldrich, D5444, dilution 1:1000), anti-eIF3β (Santa Cruz Biotechnology, sc-374156, dilution 1:50), anti-LC3B (Novus Biologicals, NB600-1384, dilution 1:200) or phalloidin (Molecular Probes – Life Technologies)] for 1 h at 4°C, washed three times with 0.05% Tween-20 in PBS, and incubated with goat anti-rabbit-IgG antibody conjugated to Alexa Fluor 594 or 488 (Life Technologies) for 1 h at 4°C. Finally, the cells were incubated with Hoechst 33342 stain for 2 min at room temperature before observation under a ZEISS AxioImager Z1 ApoTome microscope (Obj PLAN APOCHROMAT ×40, NA 1.40 oil immersion; Filter Sets FS49-DAPI, FS38-FITC and FS43-TexasRed).

Immunoprecipitations

6CFSMEO- cells were lysed in lysis buffer [1% Triton X-100, 150 mM NaCl, 10 mM Tris-HCl pH 7.4, 1 mM EDTA pH 8.0, 1 mM EGTA pH 8.0, 0.2 mM sodium orthovanadate, 0.5% NP-40, Halt™ protease, phosphatase inhibitor cocktail (Thermo Scientific)]. To eliminate nonspecific interactions, protein G (for mouse antibody) and A (for rabbit antibody) agarose beads were added to the cell extracts and incubated for 30 min at 4°C. The cell extracts were then incubated with mouse anti-actin antibody (Abcam, ab3280, dilution 1:1000) or rabbit tubulin antibody (Epitomics, PM054, dilution 1:1000). After 2 h at 4°C protein G and A agarose beads were added to the cell extracts and incubated for 2 h at 4°C. The beads were then washed four times with lysis buffer before eluting proteins from beads with 2× sample loading buffer.

Knockdown with siRNA

ICAFectin™ 442 reagent (In Cell Art, Nantes, France) was used to transfect 6CFSMEO- cells with 100 nM siRNA [siRNA control (Eurogentec), siRNA UPF1 (5'-AAGATGCAGTTCGCTCCATTTT-3'), siRNA UPF2 (5'-GAAGTTGGTACGGGCTACTC-3'), siRNA UPF3X (5'-GGAGAAGCG-AGTAACCCTG-3') (Sigma Aldrich) or siRNA actin (5'-CCCACAACG-TGCCCATTTA-3') (Thermo Scientific)], and pCMV-GPX1 Norm or pYFP-GPx1 Ter. At 24 h post transfection, the cells were incubated with DMSO or with 1 μM cytochalasin D or G418 for an additional 48 h.

Image analysis

Images were analyzed with the ImageJ software (NIH). Spots from green and red channels were detected using a local maxima detection and thresholding plugin, and counted using a particle analysis function. Logical combination of obtained masks enabled further counting of spots showing both red and green fluorescence.

Translation efficiency

6CFSMEO- cells were incubated with DMSO, 1 μM cytochalasin D, 1 μM JPK, 10 μM colchicine or 1 μM Taxotere for 48 h or with 200 μg/ml cycloheximide (as a positive control) for 4 h before harvest. Cells were then treated as previously described (Gonzalez-Hilarion et al., 2012).

Cell viability and apoptosis rate measurements

Cell viability and the apoptosis rate were measured as previously described (Jia et al., 2015).

Fluorescence *in situ* hybridization assays

6CFSMEO- cells were transfected with construct pCMV-GPx1 Ter and constructs expressing YFP-UPF1 or YFP-UPF3X. After 24 h, the cells were exposed to DMSO, 1 μM cytochalasin D, 1 μM JPK, 10 μM colchicine or 1 μM Taxotere for 48 h and then fixed in 10% formalin solution for 10 min at room temperature and permeabilized in 70% ethanol at 4°C for 1 h. The cells were then washed twice with 2× SSC before exposure to prehybridization buffer (125 μg/ml tRNA, 500 μg/ml herring DNA, 2×SSC, 1% BSA, 10% dextran sulfate, 50% formamide, 10 mM vanadyl ribonucleoside complexes) for 1 h at 37°C. Next, the cells were incubated in hybridization buffer (prehybridization buffer with 0.1 ng/μl Texas Red or Cy3-labeled probes; sequence, 5'-ACAGCAGGG-CTTCTATATCGGGTTCGATGTCGATGGTGCAGAAAGCGCCTG-3') overnight at 4°C, washed twice with 2× SSC containing 10% formamide and once with 2× SSC+0.1% Triton X-100, and twice with 1× SSC and finally incubated with Hoechst 33342 stain for 2 min at room temperature.

Construction of the plasmid expressing GPx1-Neptune

The GPx1Ter gene was amplified by PCR from plasmid pCMV-GPx1 Ter, with the following primers: sense, 5'-AGCCTCCGCGGCCCGAA-TTATGTCTGCTGCTCGGCTCTCCGC-3'; antisense, 5'-TCTTCGCCCTTAGACACCATGGGGTTGCTAGGCTGCTTGGACA,3'; Neptune-tag cDNA was amplified by PCR from the vector pmNeptune-N1 (generous gift from Prof. Roger Tsien, Department of Pharmacology, Howard Hughes Medical Institute Laboratories at the University of California, San Diego, USA), using the following primers: sense, 5'-TGTCACAGCAGCCTAGCAACCCCATGGTGTCTAAGGGCGAAGA-GCT-3'; antisense, 5'ATCTTATCATGTCTGGATCTTACTTGTACA-GCTCGTCCATG-3'. Both amplicons were used as templates to amplify, by PCR, the GPx1 Ter-Neptune construct. The Infusion cloning kit (Clontech, Mountain View, CA,) was then used to introduce this last amplicon into the pSTAR vector (Zeng et al., 1998) linearized with the BamHI and EcoRI restriction enzymes.

Live imaging

Live imaging was performed under a laser scanning confocal microscope (Zeiss Axio Observer Z1; LSM 880). Cells were maintained at 37°C in the incubation chamber. Images were taken in lambda mode (Scan Modul Quasar 34 channels) and Spectral Unmixing (Zen, Zeiss software) was used to separate signals of different wavelengths (corresponding, respectively, to YFP, dsRed and Neptune). Observations were made with a 63× P1N APO DIC II, NA 1.4 oil immersion objective, at the frequency of one image every 2 min.

FRAP assay

FRAP experiments were performed under a Zeiss LSM880 confocal microscope. A 488 nm argon laser was used to bleach YFP-UPF1 spots, and a 561 nm diode was used to bleach the RFP-DCP1a spots (200 iterations at 100% power). The sequence was programmed into the Zen (Zeiss) software. For each experiment, we first recorded two images, bleached the sample, and then recorded images every 2 s for at least 100 s. We imaged several cells, and in each cell, we bleached several bodies.

Sequences of images were analyzed with the ImageJ software (NIH). For each time point, we measured the mean intensity of regions of interest around GFP or RFP foci. Curves were normalized because the intensity was not exactly the same and bleaching was not total in every foci (intensity

before bleaching was set to 1, with offset at 0). The graphical representation of the curves was made with MATLAB®.

Measuring the distance between P-bodies and readthrough bodies

Distance analysis was performed with ImageJ. A script was written to measure, for each green foci, the distance of the nearest red foci (available upon request). To do this, we first needed to threshold the images to obtain binary masks of green and red foci. Then, we drew regions of interest with increasing diameters around the different green body. By successive measurements, we determined at which diameter of the region of interest a red body appeared. We analyzed several foci for each condition, and a boxplot representation of the results was made with MATLAB®.

Acknowledgements

The authors wish to thank Prof. Lynne Maquat, Prof. Wanjin Hong, Dr Roger Y. Tsien, Prof. Pascale Fanen, Dr Laurent Héliot, Dr Edouard Bertrand and Dr James Stévenin for reagents and Prof. Yves Lemoine and Prof. Alex Duval for helpful discussions. The authors thank the Bioluminescence Center Lille for access to instruments. We dedicate this article to the memory of Prof. Dieter C. Gruenert.

Competing interests

The authors declare no competing or financial interests.

Author contributions

Conceptualization: J.J., S.G.-H., E.W., D.C.G., F. Lejeune; Methodology: J.J., S.G.-H., E.W., F. Lejeune; Software: E.W.; Formal analysis: E.W., D.C.G., F. Lejeune; Investigation: J.J., S.G.-H., E.W., F. Lejeune; Writing - original draft: D.C.G., F. Lejeune; Writing - review & editing: J.J., S.G.-H., E.W., F. Lafont, D.T., F. Lejeune; Supervision: F. Lafont, F. Lejeune; Project administration: F. Lejeune; Funding acquisition: F. Lafont, D.C.G., D.T., F. Lejeune

Funding

J.J. received funding from the Association Française contre les Myopathies and from Association Vaincre la Mucoviscidose. F. Lejeune is an Institut National de la Santé et de la Recherche Médicale (INSERM) researcher, and received funding for this project from Association Vaincre la Mucoviscidose, Association Française contre les Myopathies, Cancéropôle Nord Ouest and Fondation ARC pour la Recherche sur le Cancer. D.C.G. was supported by funds from Pennsylvania Cystic Fibrosis Inc., Cystic Fibrosis Research Inc. and the National Institutes of Health (grant DK104681). Deposited in PMC for release after 12 months.

Supplementary information

Supplementary information available online at <http://jcs.biologists.org/lookup/doi/10.1242/jcs.198176.supplemental>

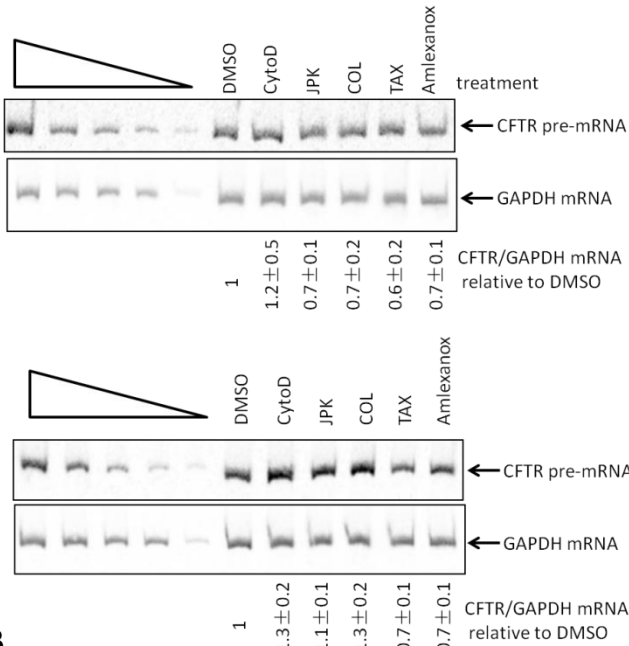
References

- Aizer, A., Kalo, A., Kafri, P., Shraga, A., Ben-Yishay, R., Jacob, A., Kinor, N. and Shav-Tal, Y. (2014). Quantifying mRNA targeting to P-bodies in living human cells reveals their dual role in mRNA decay and storage. *J. Cell Sci.* **127**, 4443–4456.
- Anczuków, O., Ware, M. D., Buisson, M., Zetoune, A. B., Stoppa-Lyonnet, D., Sinilnikova, O. M. and Mazoyer, S. (2008). Does the nonsense-mediated mRNA decay mechanism prevent the synthesis of truncated BRCA1, CHK2, and p53 proteins? *Hum. Mutat.* **29**, 65–73.
- Andrei, M. A., Ingelfinger, D., Heintzmann, R., Achsel, T., Rivera-Pomar, R. and Lührmann, R. (2005). A role for eIF4E and eIF4E-transporter in targeting mRNPs to mammalian processing bodies. *RNA* **11**, 717–727.
- Aylett, C. H. S., Löwe, J. and Amos, L. A. (2011). New insights into the mechanisms of cytomotive actin and tubulin filaments. *Int. Rev. Cell Mol. Biol.* **292**, 1–71.
- Bassell, G. J., Oleynikov, Y. and Singer, R. H. (1999). The travels of mRNAs through all cells large and small. *FASEB J.* **13**, 447–454.
- Brown, J. A. L., Roberts, T. L., Richards, R., Woods, R., Birrell, G., Lim, Y. C., Ohno, S., Yamashita, A., Abraham, R. T., Gueven, N. et al. (2011). A novel role for hSMG-1 in stress granule formation. *Mol. Cell Biol.* **31**, 4417–4429.
- Chang, Y.-F., Imam, J. S. and Wilkinson, M. F. (2007). The nonsense-mediated decay RNA surveillance pathway. *Annu. Rev. Biochem.* **76**, 51–74.
- Correa-Cerro, L. S., Wassif, C. A., Wayne, J. S., Krakowiak, P. A., Cozma, D., Dobson, N. R., Levin, S. W., Anadiotis, G., Steiner, R. D., Krajewska-Walasek, M. et al. (2005). DHCR7 nonsense mutations and characterisation of mRNA nonsense mediated decay in Smith-Lemli-Opitz syndrome. *J. Med. Genet.* **42**, 350–357.
- Cougot, N., Babajko, S. and Seraphin, B. (2004). Cytoplasmic foci are sites of mRNA decay in human cells. *J. Cell Biol.* **165**, 31–40.
- Cozens, A. L., Yezzi, M. J., Chin, L., Simon, E. M., Finkbeiner, W. E., Wagner, J. A. and Gruenert, D. C. (1992). Characterization of immortal cystic fibrosis tracheobronchial gland epithelial cells. *Proc. Natl. Acad. Sci. USA* **89**, 5171–5175.
- Cozens, A. L., Yezzi, M. J., Kunzelmann, K., Ohri, T., Chin, L., Eng, K., Finkbeiner, W. E., Widdicombe, J. H. and Gruenert, D. C. (1994). CFTR expression and chloride secretion in polarized immortal human bronchial epithelial cells. *Am. J. Respir. Cell Mol. Biol.* **10**, 38–47.
- da Paula, A. C., Ramalho, A. S., Farinha, C. M., Cheung, J., Maurisse, R., Gruenert, D. C., Ousingsawat, J., Kunzelmann, K. and Amaral, M. D. (2005). Characterization of novel airway submucosal gland cell models for cystic fibrosis studies. *Cell. Physiol. Biochem.* **15**, 251–262.
- Dorad, C., de Thonel, A., Collura, A., Marisa, L., Svrcek, M., Lagrange, A., Jegou, G., Wanherdrick, K., Joly, A. L., Buhard, O. et al. (2011). Expression of a mutant HSP110 sensitizes colorectal cancer cells to chemotherapy and improves disease prognosis. *Nat. Med.* **17**, 1283–1289.
- Durand, S., Cougot, N., Mahuteau-Betzer, F., Nguyen, C.-H., Grierson, D. S., Bertrand, E., Tazi, J. and Lejeune, F. (2007). Inhibition of nonsense-mediated mRNA decay (NMD) by a new chemical molecule reveals the dynamic of NMD factors in P-bodies. *J. Cell Biol.* **178**, 1145–1160.
- Farinha, C. M., Mendes, F., Roxo-Rosa, M., Penque, D. and Amaral, M. D. (2004). A comparison of 14 antibodies for the biochemical detection of the cystic fibrosis transmembrane conductance regulator protein. *Mol. Cell. Probes* **18**, 235–242.
- Fatscher, T., Boehm, V. and Gehring, N. H. (2015). Mechanism, factors, and physiological role of nonsense-mediated mRNA decay. *Cell. Mol. Life Sci.* **72**, 4523–4544.
- Fletcher, D. A. and Mullins, R. D. (2010). Cell mechanics and the cytoskeleton. *Nature* **463**, 485–492.
- Gatti, R. A. (2012). SMRT compounds correct nonsense mutations in primary immunodeficiency and other genetic models. *Ann. N. Y. Acad. Sci.* **1250**, 33–40.
- Gonzalez-Hilarion, S., Beghyn, T., Jia, J., Debreuck, N., Berte, G., Mamchaoui, K., Mouly, V., Gruenert, D. C., Deprez, B. and Lejeune, F. (2012). Rescue of nonsense mutations by amlexanox in human cells. *Orphanet J. Rare Dis.* **7**, 58.
- Harger, J. W. and Dinman, J. D. (2004). Evidence against a direct role for the UbF proteins in frameshifting or nonsense codon readthrough. *RNA* **10**, 1721–1729.
- He, F., Li, X., Spatrick, P., Casillo, R., Dong, S. and Jacobson, A. (2003). Genome-wide analysis of mRNAs regulated by the nonsense-mediated and 5' to 3' mRNA decay pathways in yeast. *Mol. Cell* **12**, 1439–1452.
- Hug, N., Longman, D. and Cáceres, J. F. (2016). Mechanism and regulation of the nonsense-mediated decay pathway. *Nucleic Acids Res.* **44**, 1483–1495.
- Ingelfinger, D., Arndt-Jovin, D. J., Luhrmann, R. and Achsel, T. (2002). The human LSM1-7 proteins colocalize with the mRNA-degrading enzymes Dcp1/2 and Xrn1 in distinct cytoplasmic foci. *RNA* **8**, 1489–1501.
- Isken, O., Kim, Y. K., Hosoda, N., Mayeur, G. L., Hershey, J. W. B. and Maquat, L. E. (2008). Upf1 phosphorylation triggers translational repression during nonsense-mediated mRNA decay. *Cell* **133**, 314–327.
- Jia, J., Furlan, A., Gonzalez-Hilarion, S., Leroy, C., Gruenert, D. C., Tulasne, D. and Lejeune, F. (2015). Caspases shutdown nonsense-mediated mRNA decay during apoptosis. *Cell Death Differ.* **22**, 1754–1763.
- Karousis, E. D., Nasif, S. and Mühlemann, O. (2016). Nonsense-mediated mRNA decay: novel mechanistic insights and biological impact. *Wiley Interdiscip. Rev. RNA* **7**, 661–682.
- Kervestin, S. and Jacobson, A. (2012). NMD: a multifaceted response to premature translational termination. *Nat. Rev. Mol. Cell Biol.* **13**, 700–712.
- Kuzmiak, H. A. and Maquat, L. E. (2006). Applying nonsense-mediated mRNA decay research to the clinic: progress and challenges. *Trends Mol. Med.* **12**, 306–316.
- Lejeune, F. (2017). Nonsense-mediated mRNA decay at the crossroads of many cellular pathways. *BMB Rep.*
- Lelivelt, M. J. and Culbertson, M. R. (1999). Yeast Upf proteins required for RNA surveillance affect global expression of the yeast transcriptome. *Mol. Cell Biol.* **19**, 6710–6719.
- Lopez de Heredia, M. and Jansen, R.-P. (2004). mRNA localization and the cytoskeleton. *Curr. Opin. Cell Biol.* **16**, 80–85.
- Loughran, G., Chou, M.-Y., Ivanov, I. P., Jungreis, I., Kellis, M., Kiran, A. M., Baranov, P. V. and Atkins, J. F. (2014). Evidence of efficient stop codon readthrough in four mammalian genes. *Nucleic Acids Res.* **42**, 8928–8938.
- Lykke-Andersen, J., Shu, M.-D. and Steitz, J. A. (2000). Human Upf proteins target an mRNA for nonsense-mediated decay when bound downstream of a termination codon. *Cell* **103**, 1121–1131.
- Manuvakhova, M., Keeling, K. and Bedwell, D. M. (2000). Aminoglycoside antibiotics mediate context-dependent suppression of termination codons in a mammalian translation system. *RNA* **6**, 1044–1055.
- Mendell, J. T., ap Rhys, C. M. and Dietz, H. C. (2002). Separable roles for rent1/hUpf1 in altered splicing and decay of nonsense transcripts. *Science* **298**, 419–422.
- Mendell, J. T., Sharifi, N. A., Meyers, J. L., Martinez-Murillo, F. and Dietz, H. C. (2004). Nonsense surveillance regulates expression of diverse classes of mammalian transcripts and mutates genomic noise. *Nat. Genet.* **36**, 1073–1078.
- Moriarty, P. M., Reddy, C. C. and Maquat, L. E. (1998). Selenium deficiency reduces the abundance of mRNA for Se-dependent glutathione peroxidase 1 by a

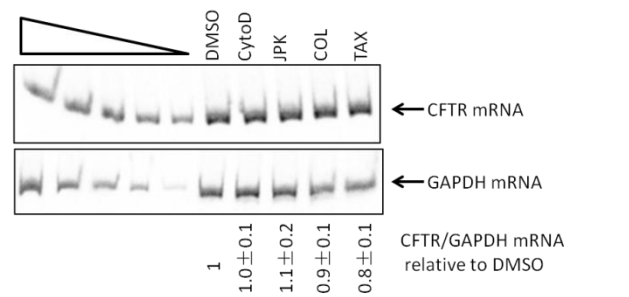
- UGA-dependent mechanism likely to be nonsense codon-mediated decay of cytoplasmic mRNA. *Mol. Cell. Biol.* **18**, 2932-2939.
- Mühlemann, O. and Lykke-Andersen, J.** (2010). How and where are nonsense mRNAs degraded in mammalian cells? *RNA Biol.* **7**, 28-32.
- Popp, M. W.-L. and Maquat, L. E.** (2014). The dharma of nonsense-mediated mRNA decay in mammalian cells. *Mol. Cells* **37**, 1-8.
- Popp, M. W. and Maquat, L. E.** (2015). Attenuation of nonsense-mediated mRNA decay facilitates the response to chemotherapeutics. *Nat. Commun.* **6**, 6632.
- Rebbapragada, I. and Lykke-Andersen, J.** (2009). Execution of nonsense-mediated mRNA decay: what defines a substrate? *Curr. Opin. Cell Biol.* **21**, 394-402.
- Rehwinkel, J., Letunic, I., Raes, J., Bork, P. and Izaurralde, E.** (2005). Nonsense-mediated mRNA decay factors act in concert to regulate common mRNA targets. *RNA* **11**, 1530-1544.
- Salas-Marco, J. and Bedwell, D. M.** (2005). Discrimination between defects in elongation fidelity and termination efficiency provides mechanistic insights into translational readthrough. *J. Mol. Biol.* **348**, 801-815.
- Serin, G., Gersappe, A., Black, J. D., Aronoff, R. and Maquat, L. E.** (2001). Identification and characterization of human orthologues to *Saccharomyces cerevisiae* Upf2 protein and Upf3 protein (*Caenorhabditis elegans* SMG-4). *Mol. Cell. Biol.* **21**, 209-223.
- Shalev, M., Kandasamy, J., Skalka, N., Belakhov, V., Rosin-Arbesfeld, R. and Baasov, T.** (2013). Development of generic immunoassay for the detection of a series of aminoglycosides with 6'-OH group for the treatment of genetic diseases in biological samples. *J. Pharm. Biomed. Anal.* **75**, 33-40.
- Sheth, U. and Parker, R.** (2003). Decapping and decay of messenger RNA occur in cytoplasmic processing bodies. *Science* **300**, 805-808.
- Singh, G., Jakob, S., Kleedehn, M. G. and Lykke-Andersen, J.** (2007). Communication with the exon-junction complex and activation of nonsense-mediated decay by human Upf proteins occur in the cytoplasm. *Mol. Cell* **27**, 780-792.
- Sureau, A., Gattoni, R., Dooghe, Y., Stévenin, J. and Soret, J.** (2001). SC35 autoregulates its expression by promoting splicing events that destabilize its mRNAs. *EMBO J.* **20**, 1785-1796.
- Tanida, I., Ueno, T. and Kominami, E.** (2008). LC3 and Autophagy. *Methods Mol. Biol.* **445**, 77-88.
- Trcek, T., Sato, H., Singer, R. H. and Maquat, L. E.** (2013). Temporal and spatial characterization of nonsense-mediated mRNA decay. *Genes Dev.* **27**, 541-551.
- Tucker, T. A., Fortenberry, J. A., Zsembery, A., Schwiebert, L. M. and Schwiebert, E. M.** (2012). The DeltaF508-CFTR mutation inhibits wild-type CFTR processing and function when co-expressed in human airway epithelia and in mouse nasal mucosa. *BMC Physiol.* **12**, 12.
- Unterholzner, L. and Izaurralde, E.** (2004). SMG7 acts as a molecular link between mRNA surveillance and mRNA decay. *Mol. Cell* **16**, 587-596.
- van Dijk, E., Cougot, N., Meyer, S., Babajko, S., Wahle, E. and Seraphin, B.** (2002). Human Dcp2: a catalytically active mRNA decapping enzyme located in specific cytoplasmic structures. *EMBO J.* **21**, 6915-6924.
- Viegas, M. H., Gehring, N. H., Breit, S., Hentze, M. W. and Kulozik, A. E.** (2007). The abundance of RNPS1, a protein component of the exon junction complex, can determine the variability in efficiency of the Nonsense Mediated Decay pathway. *Nucleic Acids Res.* **35**, 4542-4551.
- Wang, W., Czaplinski, K., Rao, Y. and Peltz, S. W.** (2001). The role of Upf proteins in modulating the translation read-through of nonsense-containing transcripts. *EMBO J.* **20**, 880-890.
- Welch, E. M., Barton, E. R., Zhuo, J., Tomizawa, Y., Friesen, W. J., Trifillis, P., Paushkin, S., Patel, M., Trotta, C. R., Hwang, S. et al.** (2007). PTC124 targets genetic disorders caused by nonsense mutations. *Nature* **447**, 87-91.
- Yamashita, A., Izumi, N., Kashima, I., Ohnishi, T., Saari, B., Katsuhata, Y., Muramatsu, R., Morita, T., Iwamatsu, A., Hachiya, T. et al.** (2009). SMG-8 and SMG-9, two novel subunits of the SMG-1 complex, regulate remodeling of the mRNA surveillance complex during nonsense-mediated mRNA decay. *Genes Dev.* **23**, 1091-1105.
- You, K. T., Li, L. S., Kim, N.-G., Kang, H. J., Koh, K. H., Chwae, Y.-J., Kim, K. M., Kim, Y. K., Park, S. M., Jang, S. K. et al.** (2007). Selective translational repression of truncated proteins from frameshift mutation-derived mRNAs in tumors. *PLoS Biol.* **5**, e109.
- Zeng, Q., Tan, Y. H. and Hong, W.** (1998). A single plasmid vector (pSTAR) mediating efficient tetracycline-induced gene expression. *Anal. Biochem.* **259**, 187-194.

Supplemental figure S1

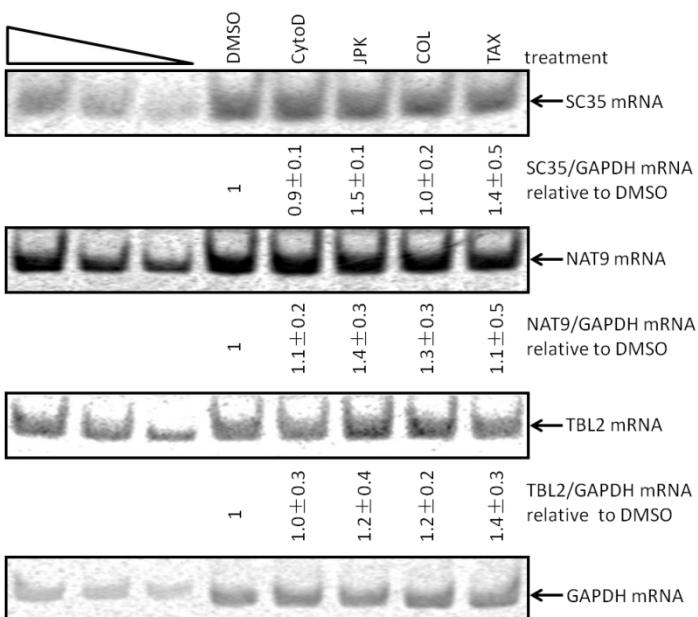
A.



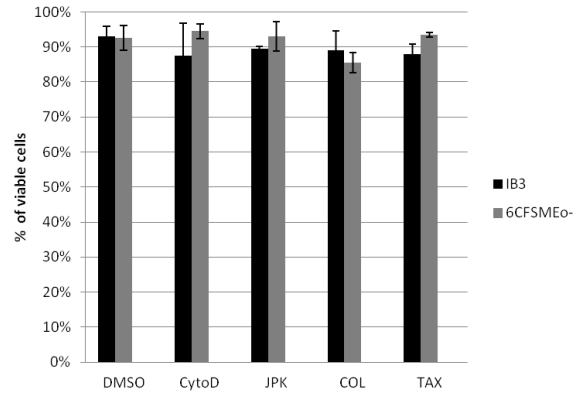
B.



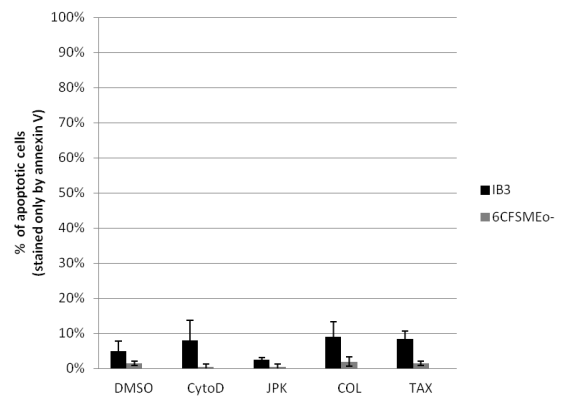
E.



C.



D.



F.

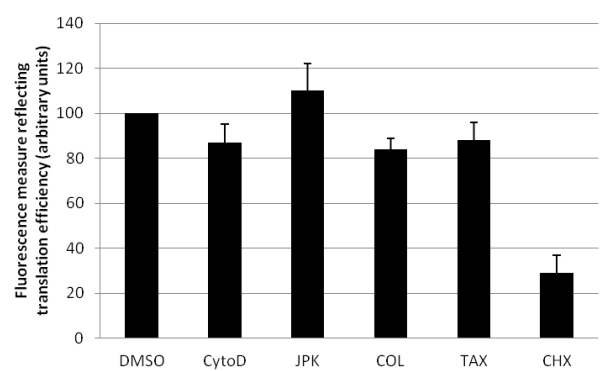
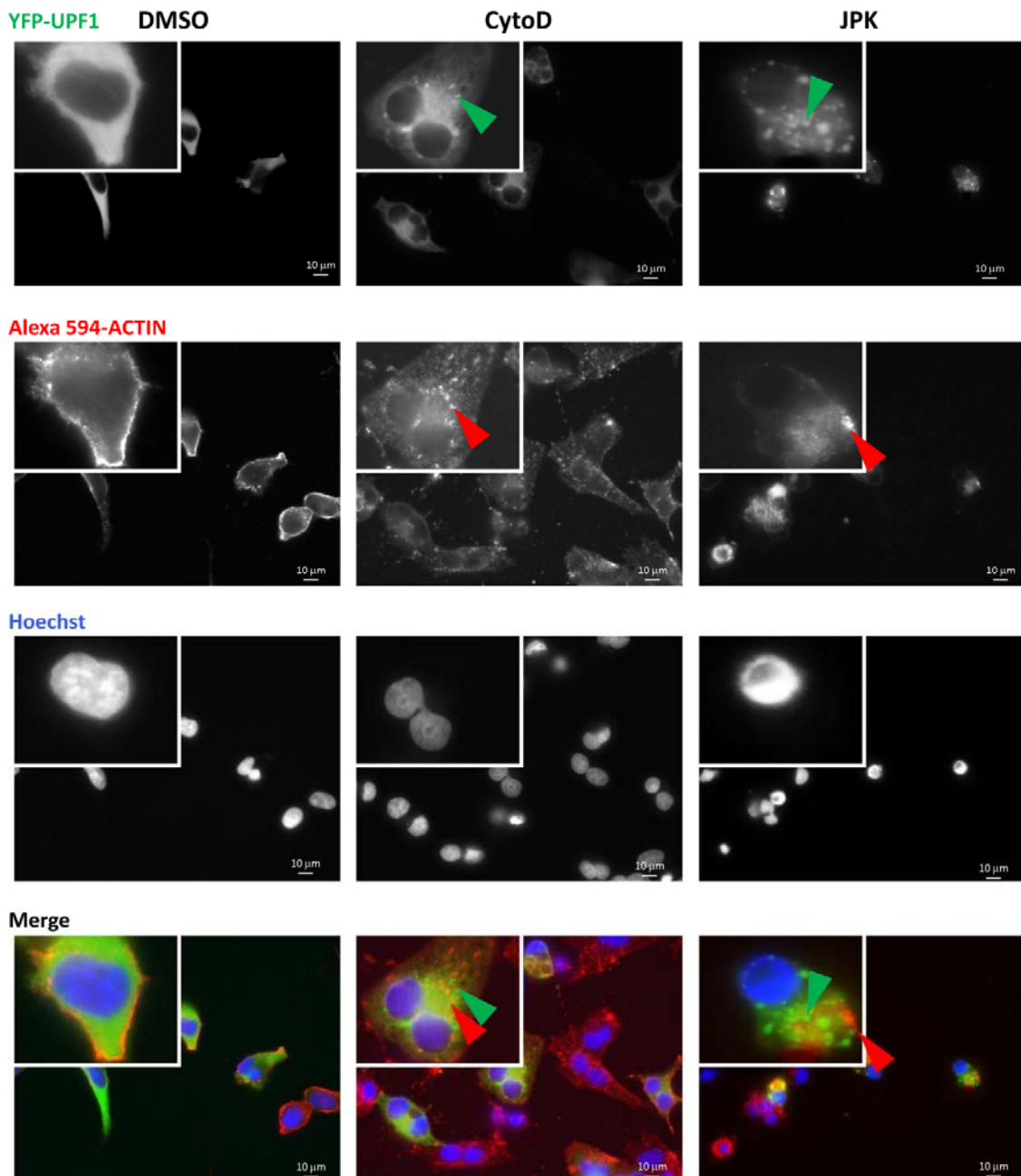
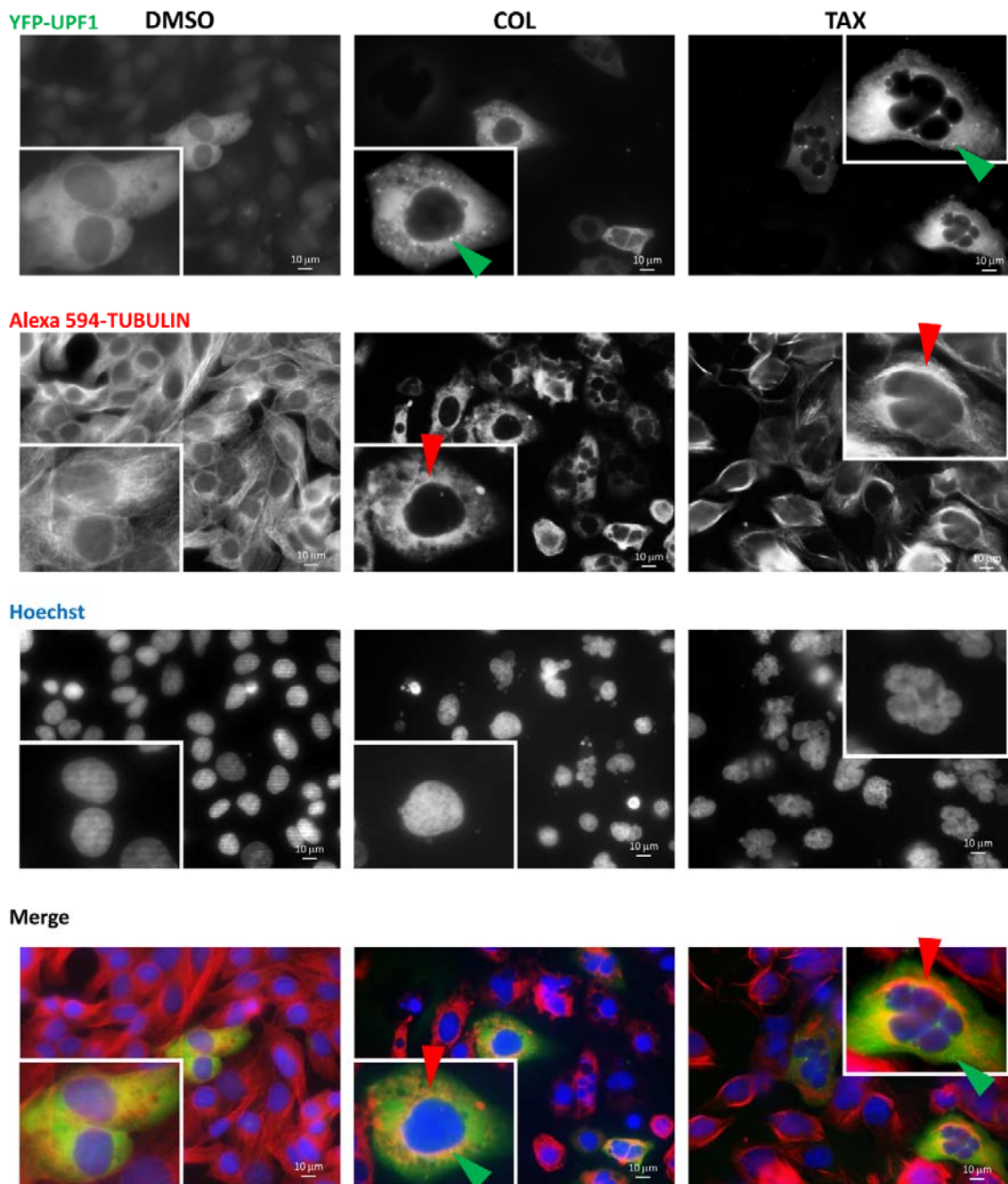


Figure S1: Effect of cytoskeleton inhibitors on some gene expression parameters. (A and B) Cytoskeleton inhibitors do not interfere with transcription or with expression of the CFTR gene. 6CFSMEo- (A upper panels) and IB3 (A lower panels) cells were incubated with DMSO, CytoD, JPK, COL, TAX, or amlexanox for 48 h. The level of CFTR pre-mRNA was measured by RT-PCR and normalized to the level of GAPDH mRNA. (B) 16HBE14o- cells were incubated with DMSO, CytoD, JPK, COL or TAX for 48 h. The level of CFTR mRNA was measured by RT-PCR and normalized to the level of GAPDH mRNA. The five leftmost lanes represent two-fold serial dilutions of RNA from Calu3 cells overexpressing CFTR mRNA. These results combine two independent experiments. (C and D) Cytoskeleton inhibitors do not induce cell death or apoptosis in IB3 or 6CFSMEo- cells. IB3 and 6CFSMEo- cells were incubated with DMSO, CytoD, JPK, COL, or TAX for 48 h and then stained with Annexin V and propidium iodine. Cell viability (C) and the apoptosis rate (D) were then measured. These results are representative of three independent experiments. (E) Cytoskeleton inhibitors do not affect natural NMD substrates. 6CFSMEo- cells were incubated with DMSO, CytoD, JPK, COL, or TAX for 48 h. RT-PCR was performed to measure the levels of SC35 mRNA, NAT9 mRNA, and TBL2 mRNA. The mRNA levels were normalized to the level of GAPDH mRNA. The three leftmost lanes represent two-fold serial dilutions of RNA from 6CFSMEo- cells. These results are representative of three independent experiments. (F) Cytoskeleton inhibitors do not affect translation. 6CFSMEo- cells were incubated with DMSO, CytoD, JPK, COL, or TAX for 48 h or with 200 μ g/ml cycloheximide (CHX) (as positive control) for 4 h. One hour before harvest, 25 μ M L-azidohomoalanine (L-AHA) was added to the cell culture medium, to be incorporated into newly synthesized proteins. Then cells were collected and the Click-iT Protein Analysis Detection Kit (Lifetechnologies) was used to measure the translation efficiency. These results are representative of three independent experiments.

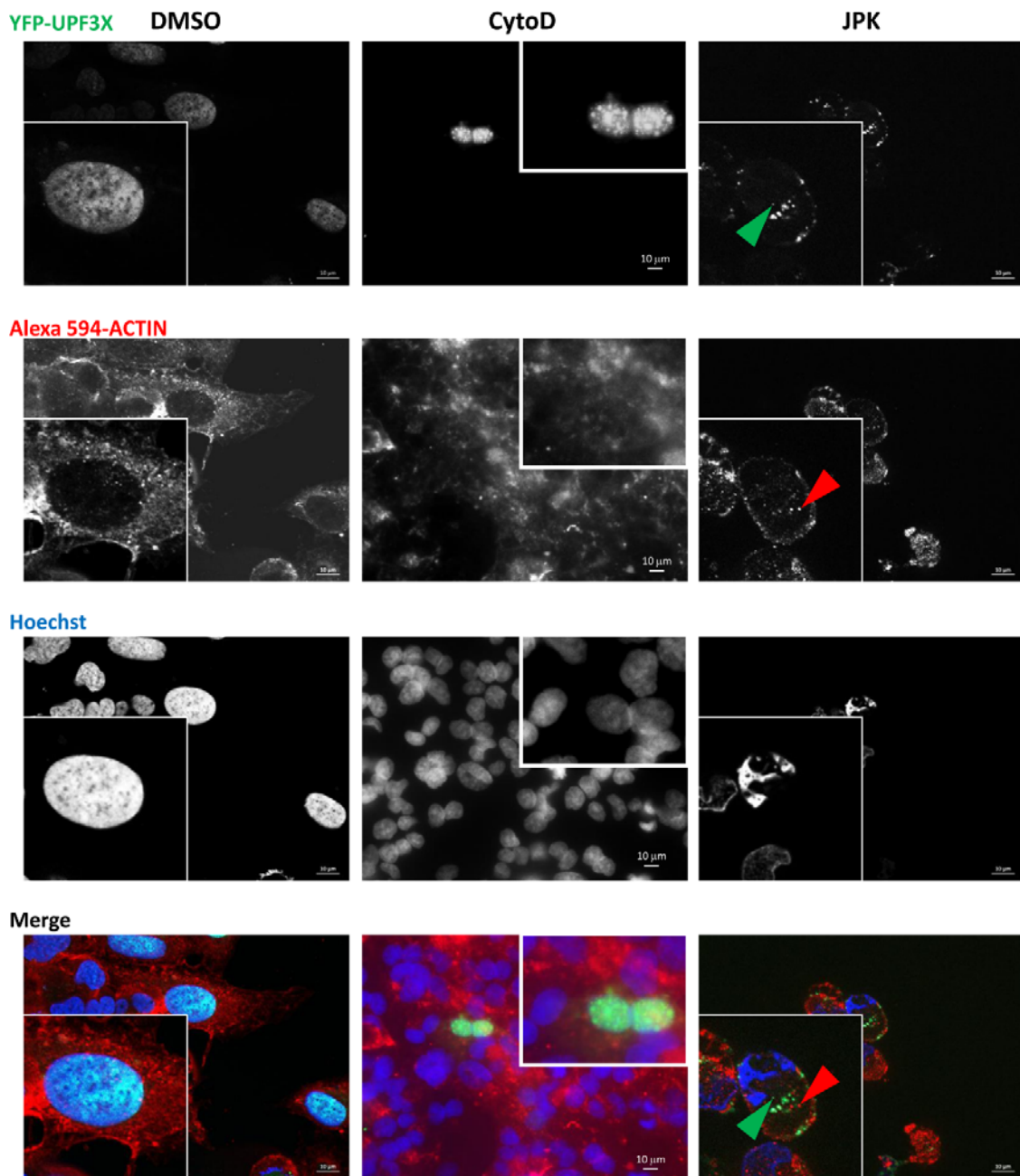
Supplemental figure S2A



Supplemental figure S2B



Supplemental figure S2C



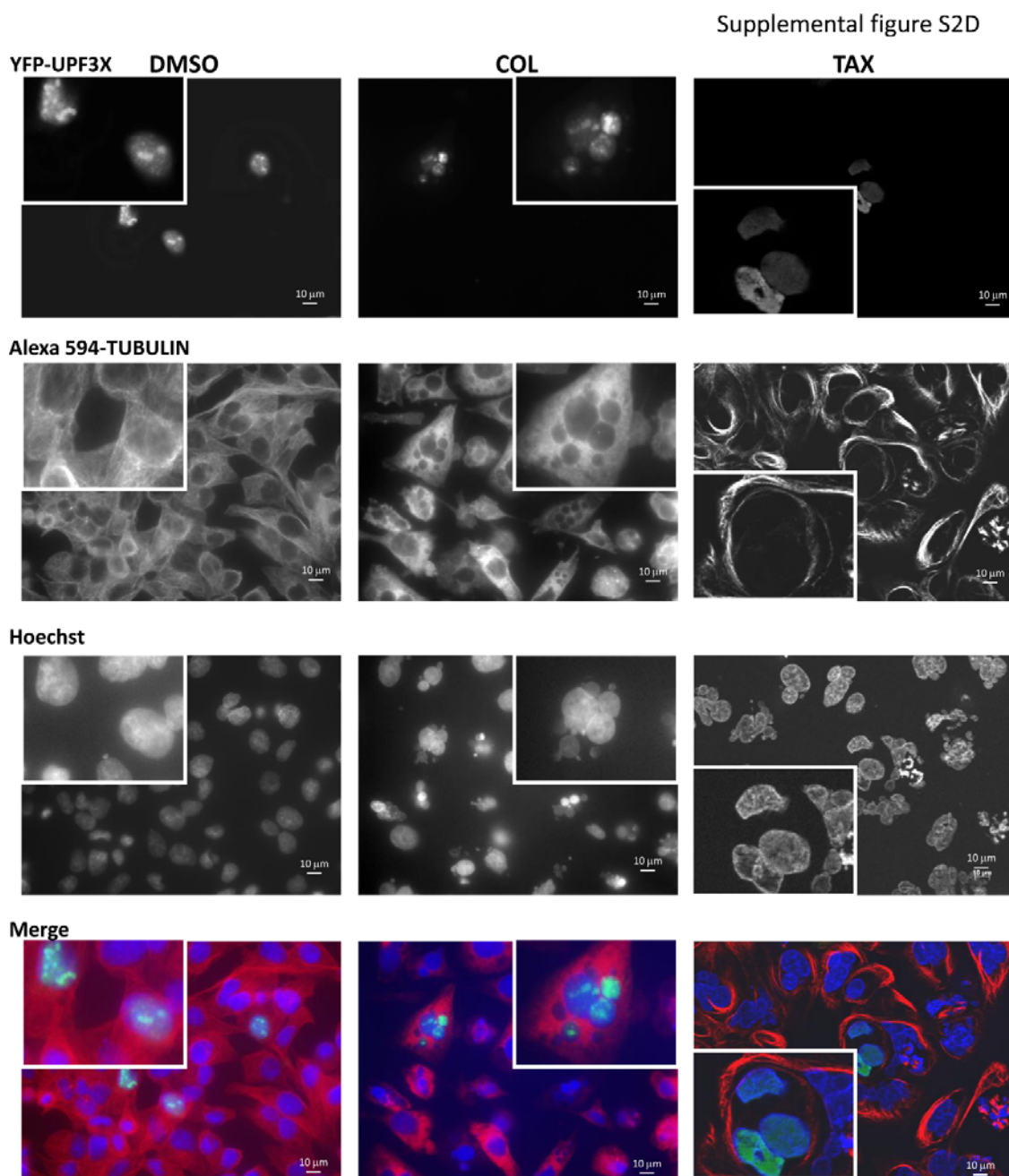


Figure S2: Cytoskeleton inhibitors affect the cellular location of NMD factors. 6CFSMEo- cells transfected with expression constructs encoding YFP-UPF1 (A and B) or YFP-UPF3X (C and D) and GPx1 46Ter were incubated with DMSO, CytoD, JPK, COL, or TAX. After 48 h, the cells were fixed, permeabilized, and incubated sequentially with primary antibodies (actin (A, C) or tubulin (B, D)) and Alexa Fluor 594 secondary antibody (red) before staining of nuclei with Hoechst stain (blue). Green arrows indicate UPF1 or UPF3X cytoplasmic foci; Red arrows indicate concentration of actin or tubulin.

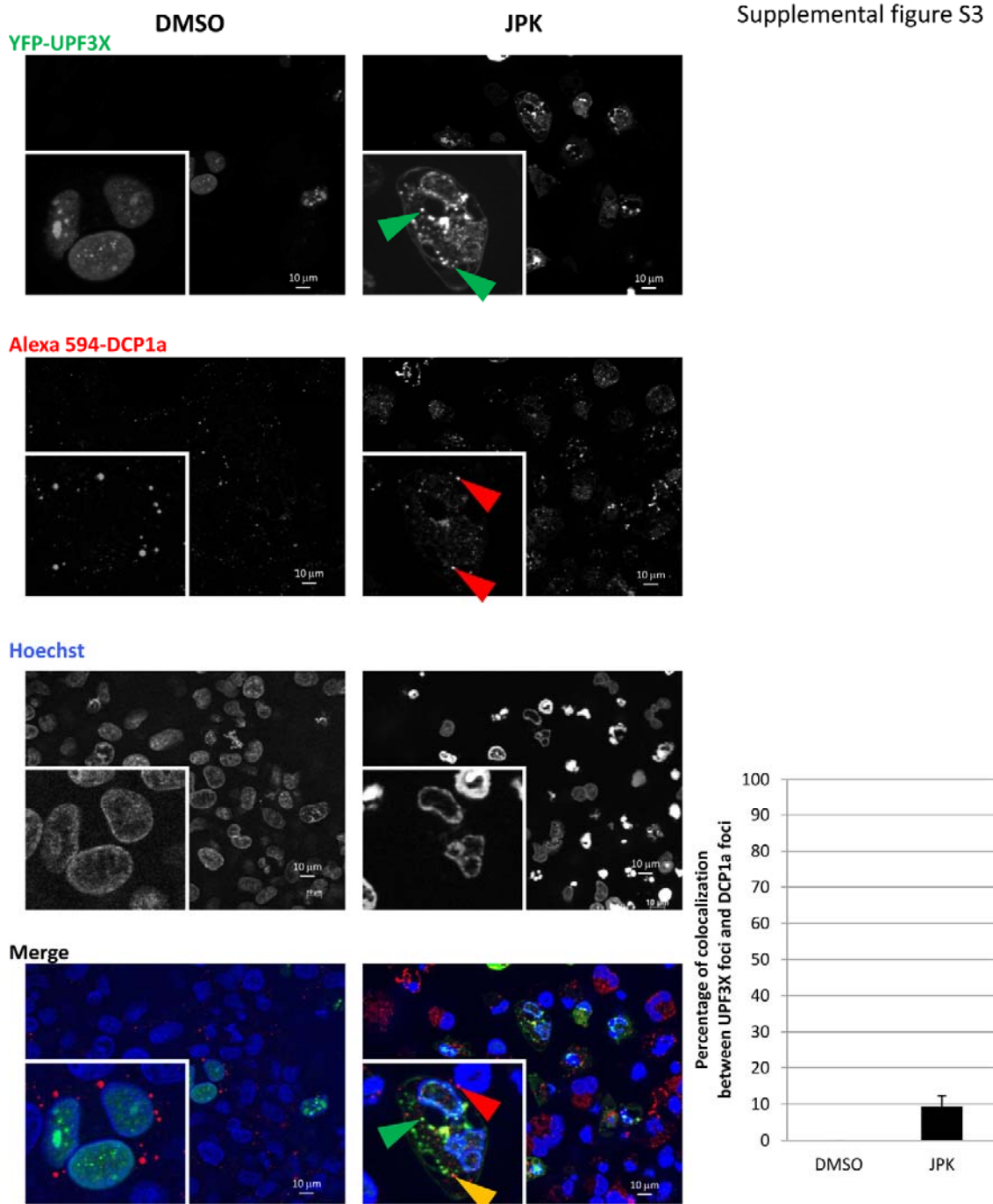


Figure S3: UPF3X concentrates partially in P-bodies under JPK treatment in 6CFSMEo- cells. Cells transfected with an expression construct encoding YFP-UPF3X or GPx1 46Ter were incubated with DMSO or JPK for 48 h. After fixation and permeabilization, the cells were incubated sequentially with anti-DCP1a primary antibody and Alexa Fluor 594 secondary antibody (red). Finally, the cells were incubated with Hoechst stain (blue) to visualize their nuclei. Green arrows indicate UPF3X cytoplasmic foci; red arrows indicate the P-body marker DCP1a; orange arrows indicate colocalization between UPF3X and DCP1a. The histogram represents the percentage of colocalization between UPF3X foci and DCP1a foci. Cells (N=10) were counted from three different experiments.

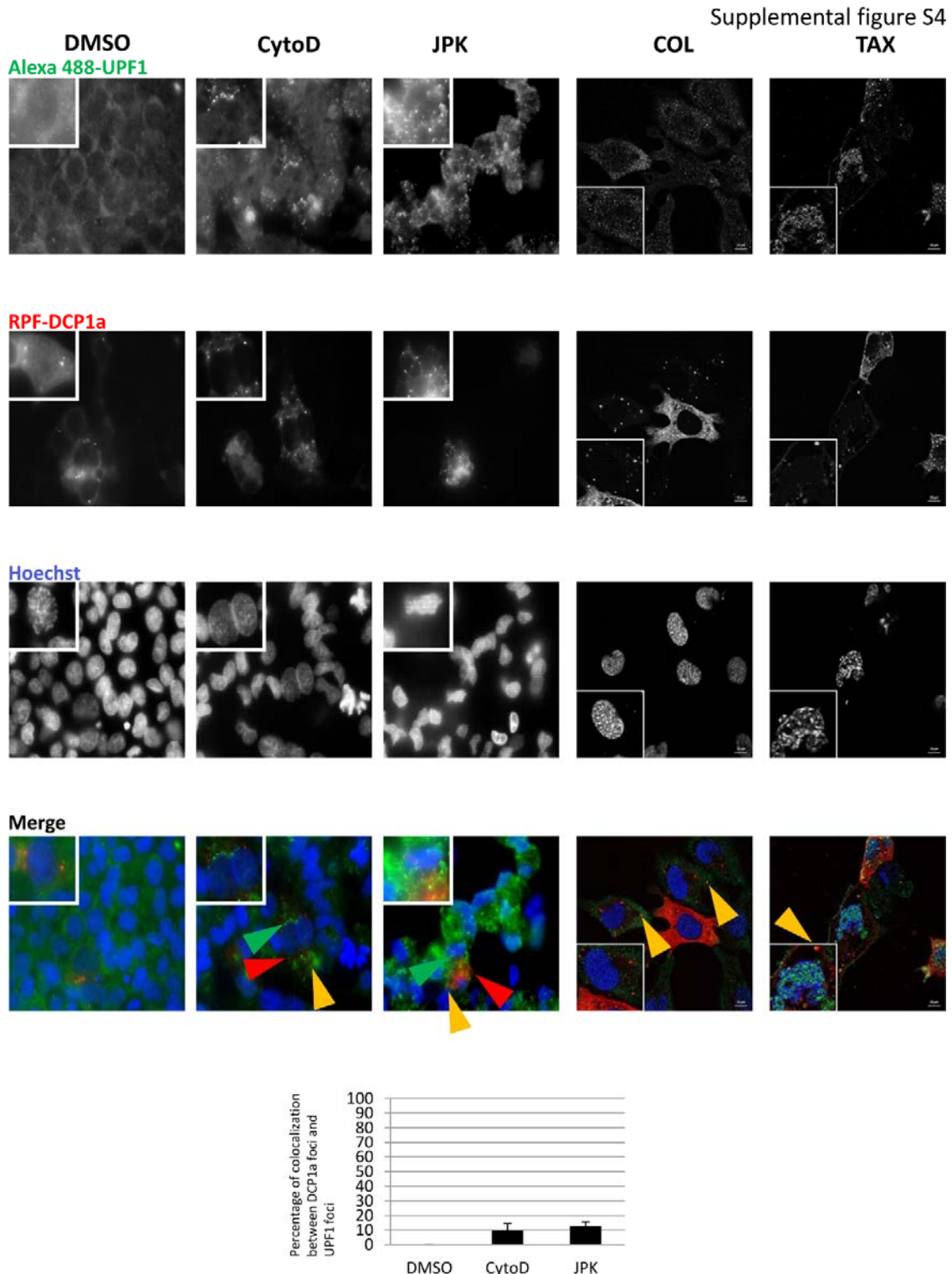


Figure S4: In 6CFSMEo- cells, endogenous UPF1 protein concentrates mainly in P-bodies upon COL or TAX treatment and only partially upon CytoD or JPK treatment. Cells were treated with DMSO, CytoD, JPK, COL, or TAX for 48 h. After fixation and permeabilization, the cells were incubated first with the anti-DCP1a or anti-UPF1 primary antibody and then with the Alexa Fluor 594 secondary antibody (red) or Alexa Fluor 488 secondary antibody (green). Finally, the nuclei were visualized in blue by Hoechst staining. Green arrows indicate UPF1 cytoplasmic foci; red arrows indicate the P-body marker DCP1a; orange arrows indicate colocalization of UPF1 and DCP1a. The histogram represents the percentage of colocalization between UPF1 foci and DCP1a foci. Cells (N=10) from three different experiments were counted for each condition.

Supplemental figure S5

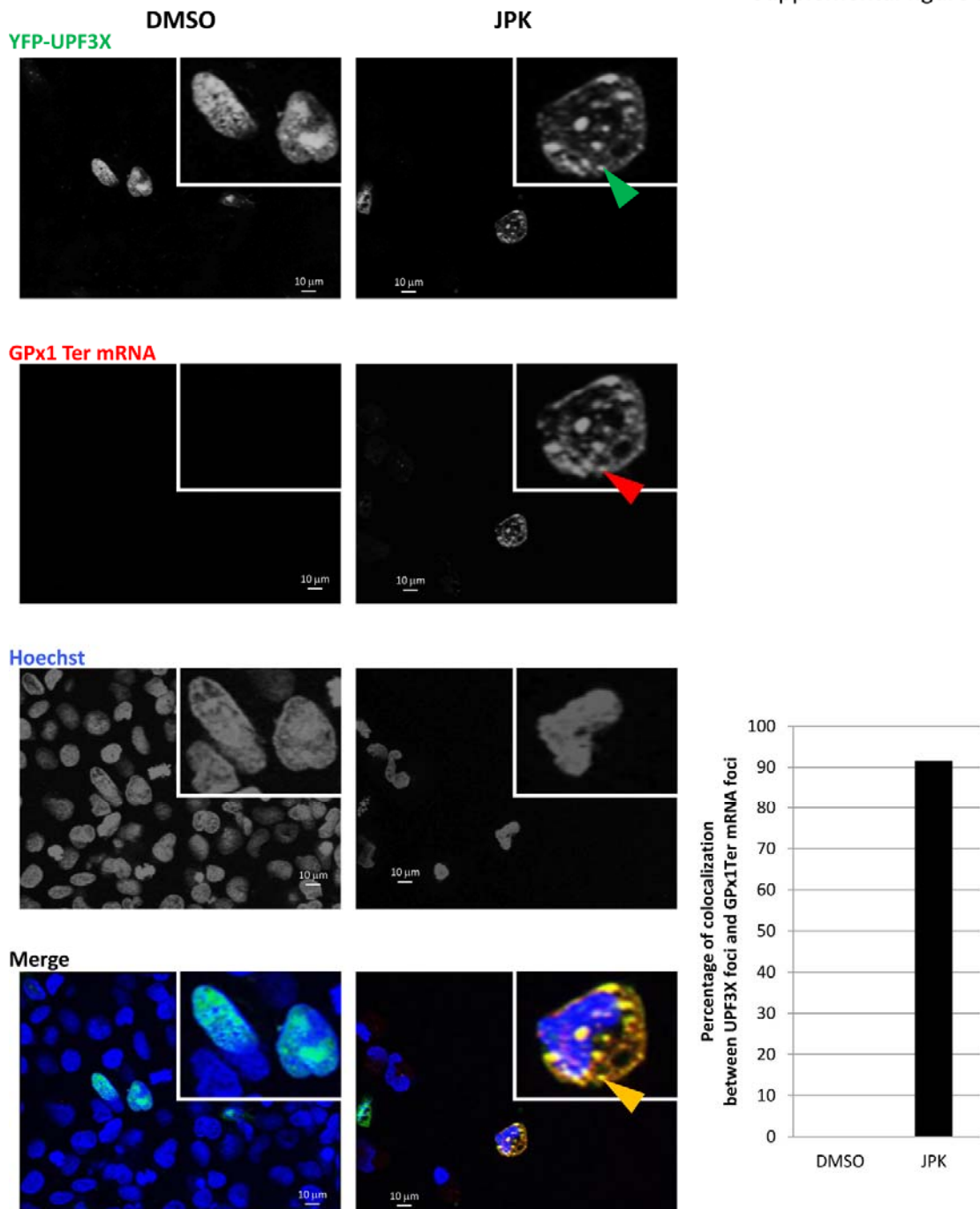
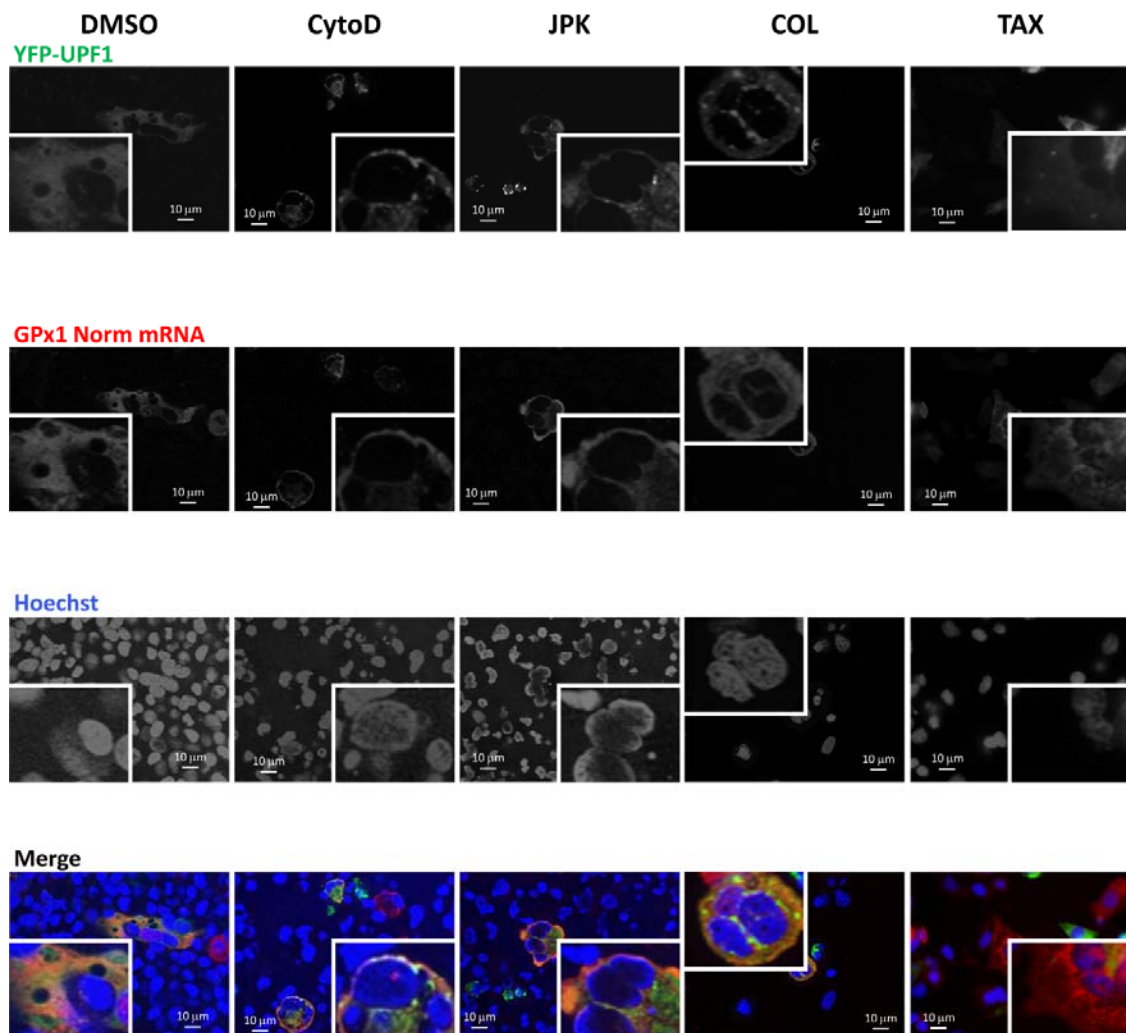


Figure S5: NMD factor UPF3X colocalizes with NMD substrates under cytoskeleton disruptor treatment in 6CFSMEo- cells. 6CFSMEo- cells were transfected with constructs expressing *GPx1 46Ter* and *YFP-UPF3X* and then incubated with DMSO, CytoD, JPK, COL, or TAX for 48 h. A FISH assay was performed to detect the cellular localization of *GPx1 46Ter* mRNA. Nuclei are stained in blue with Hoechst stain. Green arrows indicate UPF3X cytoplasmic foci; red arrows indicate *GPx1* mRNA cytoplasmic foci; orange arrows indicate colocalization of the UPF3X factor and NMD substrates.

Supplemental figure S6A



Supplemental figure S6B

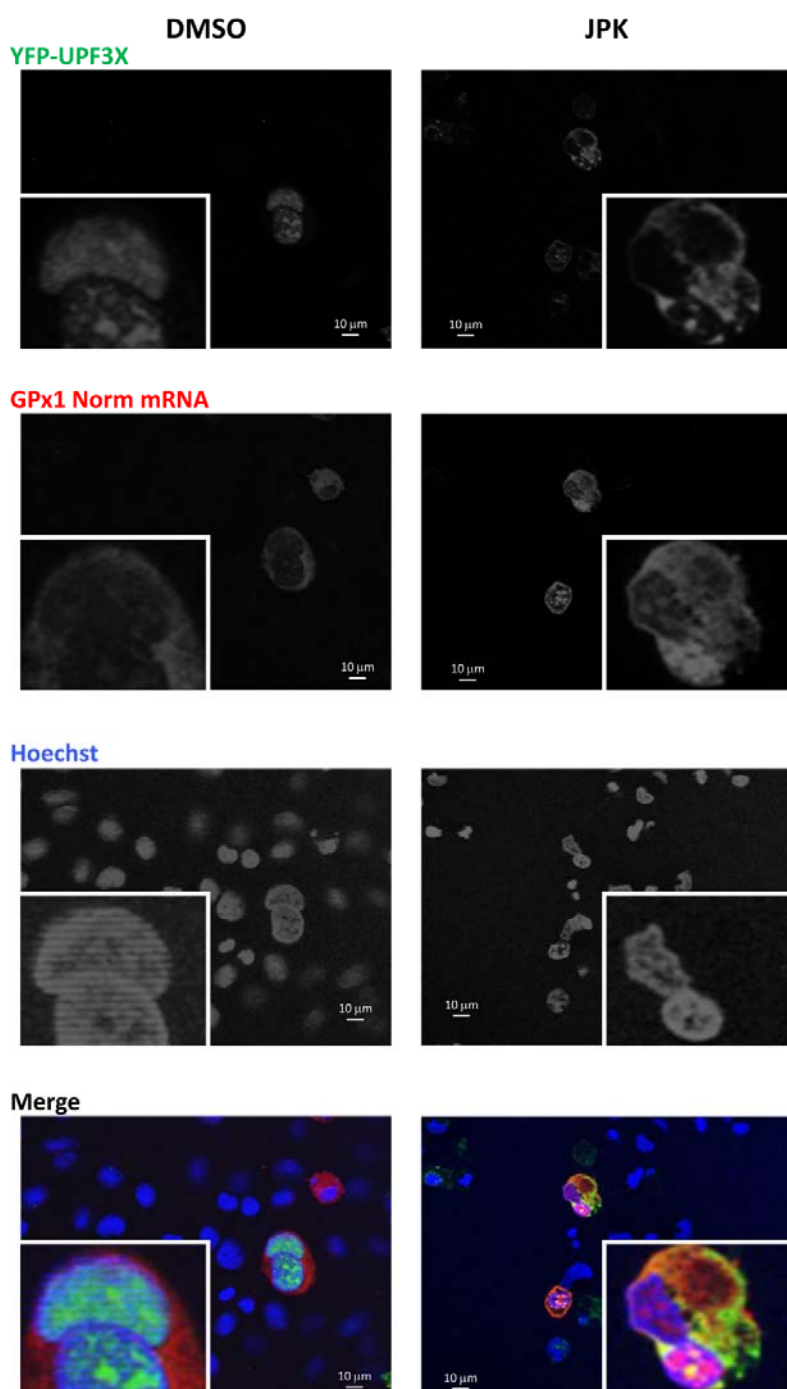


Figure S6: Cytoskeleton disruptors do not affect the cellular location of wild-type mRNAs in 6CFSMEo- cells. 6CFSMEo- cells were transiently transfected to express *GPx1 Norm* and *YFP-UPF1* (A) or *YFP-UPF3X* (B) and then incubated with DMSO, CytoD, JPK, COL, or TAX for 48 h. After fixation and permeabilization, they were incubated overnight at 37°C with Texas-red-labeled probes. Nuclei were stained with Hoechst solution (blue).

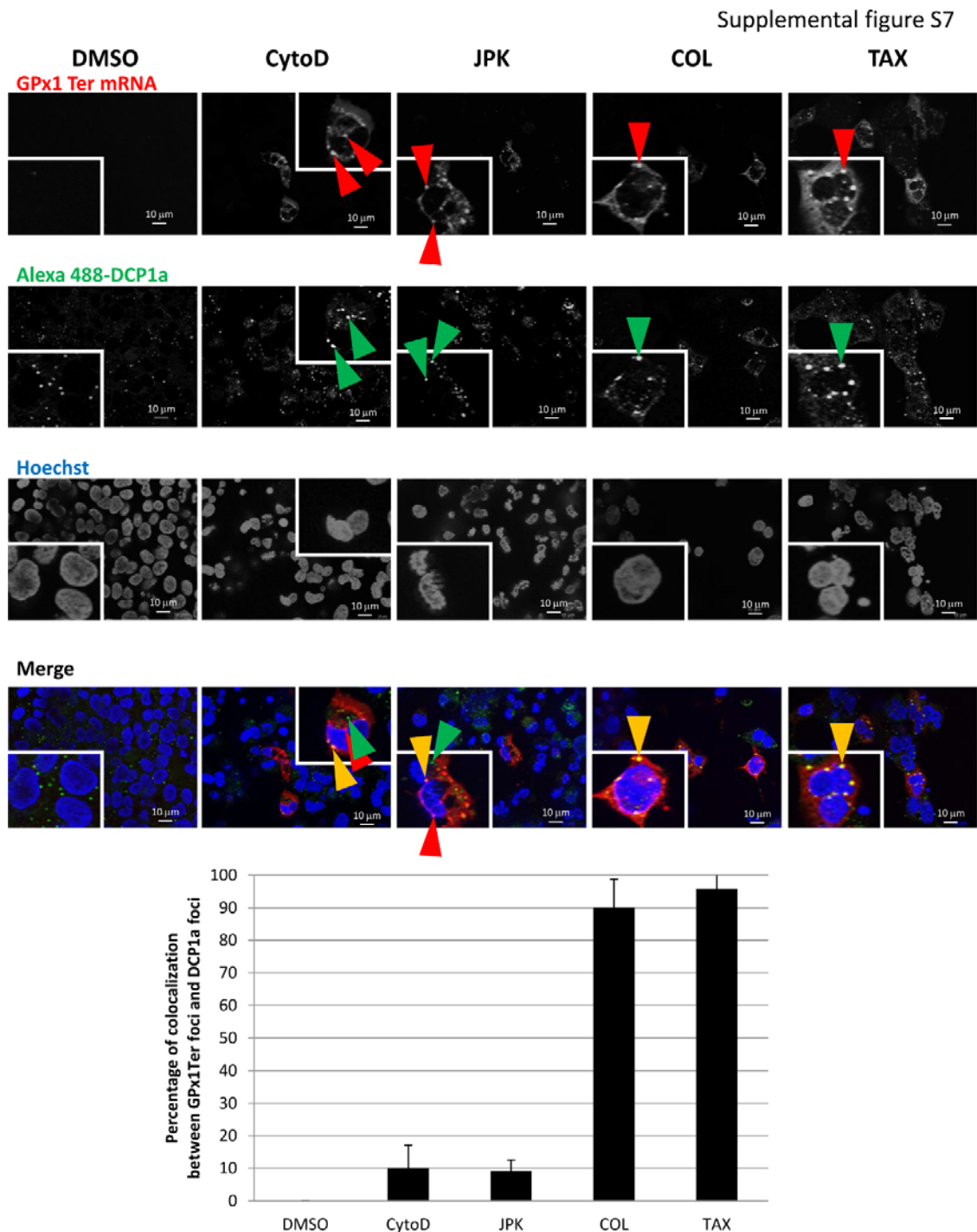
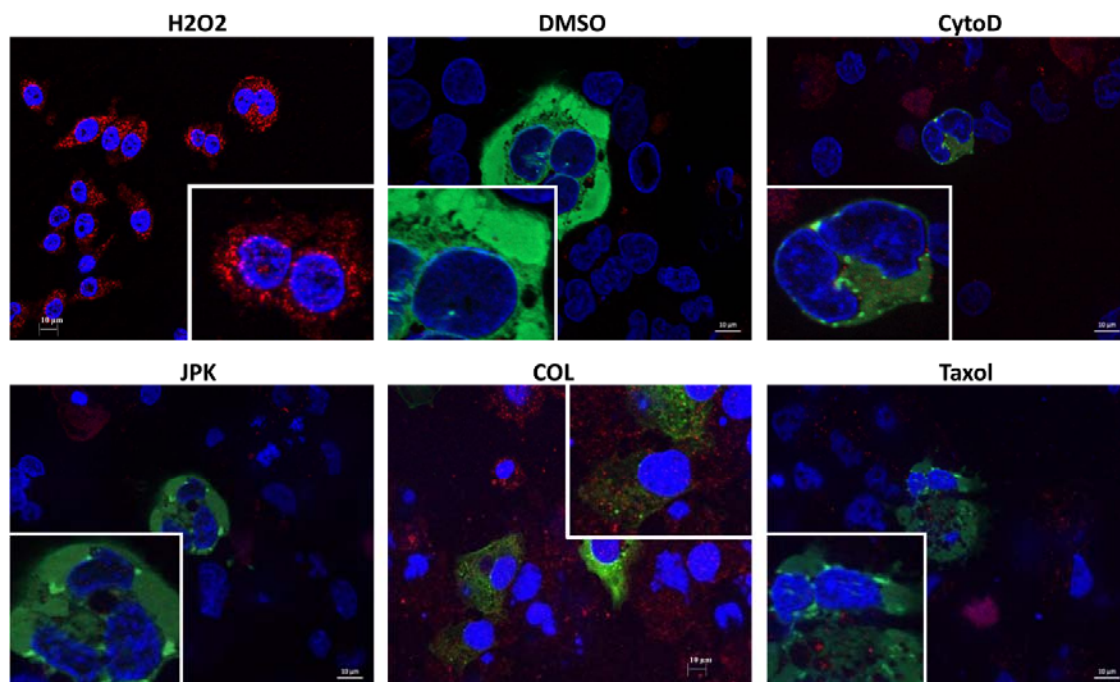


Figure S7: NMD substrates partially or totally concentrate in P-bodies under cytoskeleton disruptor treatment. 6CFSMEo- cells were transfected with constructs expressing *Flag-UPF1* and *GPx1 46Ter*. The cells were then incubated with DMSO, CytoD, JPK, COL, or TAX for 48 h. The location of GPx1 46Ter mRNA was monitored by FISH (red). The cells were then incubated sequentially with anti-DCP1a primary antibody and Alexa Fluor 488 secondary antibody (green). Nuclei were stained in blue with Hoechst solution. Green arrows indicate P-bodies; red arrows indicate GPx1-mRNA-containing cytoplasmic foci; orange arrows indicate colocalization of DCP1a and NMD substrates. The histogram represents the percentage of colocalization between GPx1 Ter mRNA and DCP1a. Cells (N=10) from three different experiments were counted for each condition.

Supplemental figure S8

A. YFP-UPF1



B. YFP-UPF3X

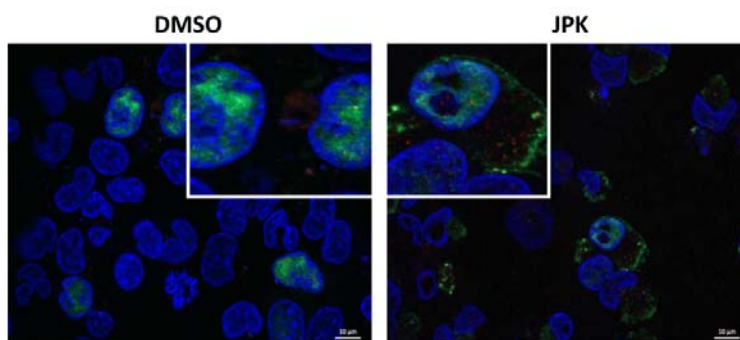
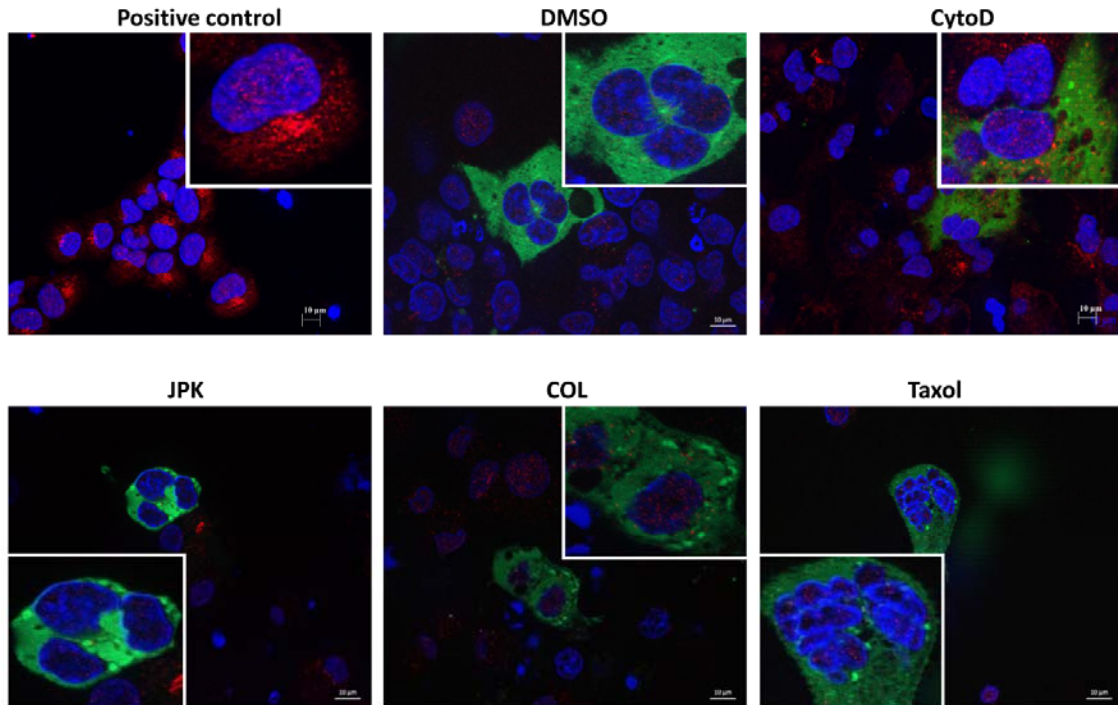


Figure S8: In 6CFSMEo-cells, NMD factors do not colocalize with stress granules upon cytoskeleton inhibitor treatment. 6CFSMEo- cells transfected with a construct expressing *YFP-UPF1* (A) or *YFP-UPF3X* (B) and the construct pCMV-GPx1 46Ter were incubated with DMSO, 1 μ M CytoD, 1 μ M JPK, 10 μ M COL, or 1 μ M Taxol for 48h. 6CFSMEo- cells treated with 1.5 mM H₂O₂ for 4 h were used as positive control. Cells were fixed and permeabilized prior to incubation for 1 h at 4°C with primary antibody against eIF3 β (a marker of stress granules), washed three times with PBS, and incubated with goat anti-rabbit antibody labeled with Alexa Fluor 594 (red). Cells were washed three times with PBS and incubated with Hoechst stain (blue) for 2 min at room temperature.

Supplemental figure S9

A. YFP-UPF1



B. YFP-UPF3X

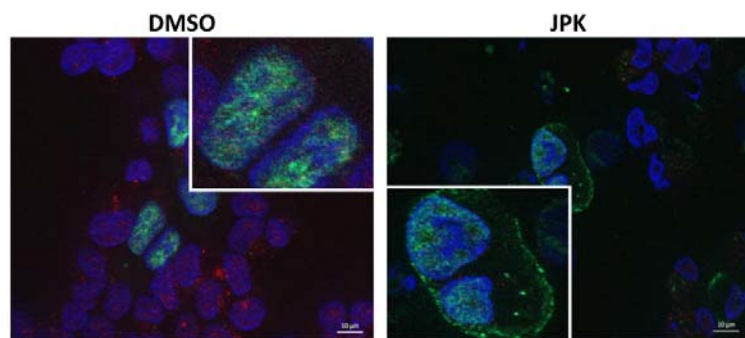


Figure S9: NMD factors do not colocalize with autophagosomes in 6CFSMEo-cells treated with cytoskeleton inhibitors. 6CFSMEo- cells transfected with a construct expressing *YFP-UPF1* (A) or *YFP-UPF3X* (B) and the construct pCMV-GPx1 Ter were incubated respectively with DMSO, 1 μ M CytoD, 1 μ M JPK, 10 μ M COL or 1 μ M Taxol for 48 h. As positive control, 6CFSMEo-cells were incubated in serum-free medium for 24 h. Cells were then fixed and permeabilized prior to incubation for 1 h at 4°C with primary antibody (anti-LC3B antibody), washed three times with PBS, and incubated with goat anti-rabbit antibody labeled with Alexa Fluor 594 (red). Cells were washed three times with PBS and incubated with Hoechst stain (blue) for 2 min at room temperature.

Supplemental figure S10

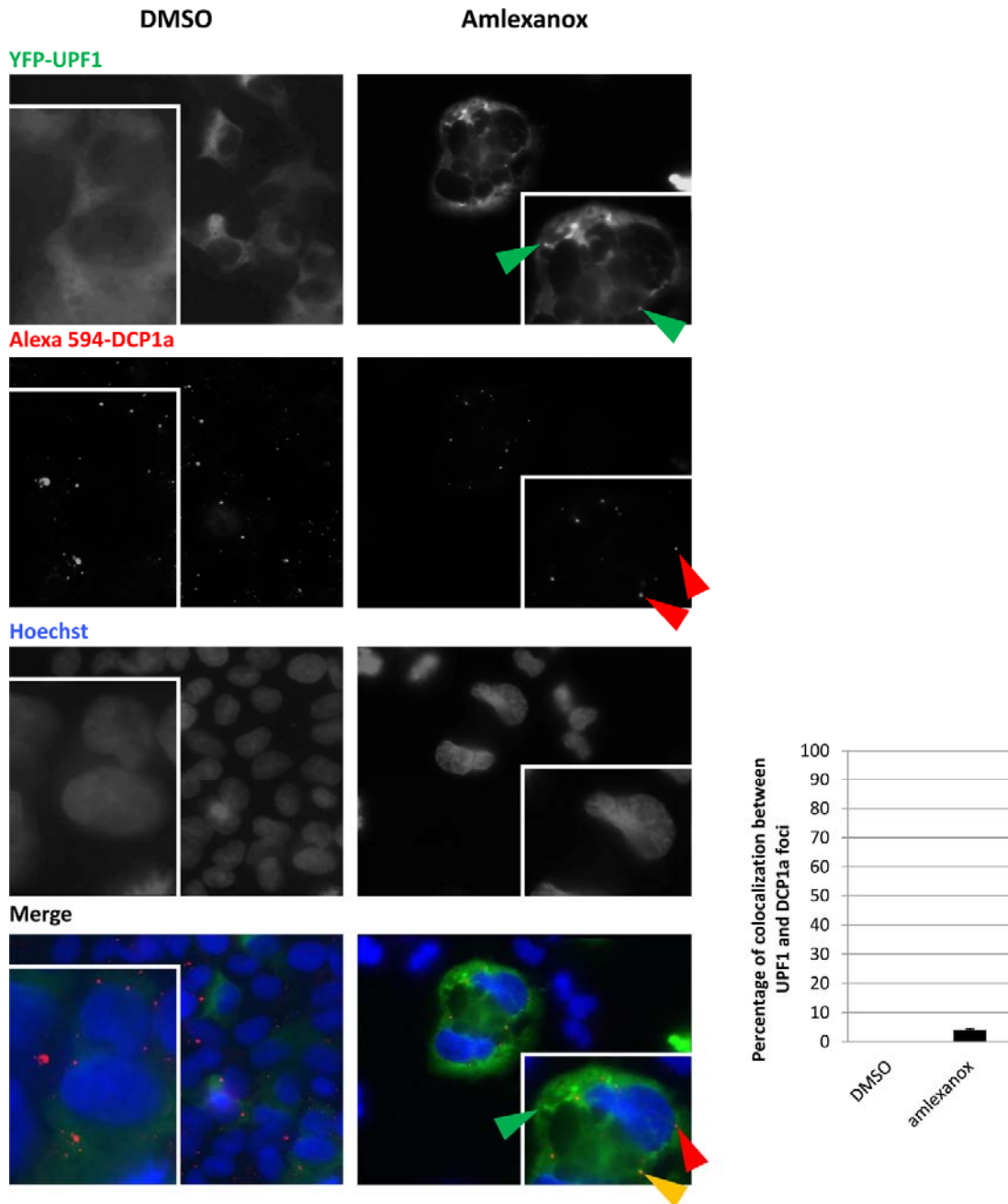


Figure S10: Amlexanox causes UPF1 to localize to cytoplasmic foci distinct from P-bodies. 6CFSMEo- cells were transfected with constructs expressing *YFP-UPF1* before treatment with DMSO (left column) or 25 μ M amlexanox (right column) for 48 h. Cells were incubated sequentially with DCP1a antibody and Alexa Fluor 594 labeled secondary antibody (red). The percentage of colocalization between UPF1 and DCP1a is presented in a histogram at the bottom of the figure. Cells (N=10) from three different experiments were counted for each condition. Nuclei were stained with Hoechst solution (blue). Green arrows indicate UPF1 cytoplasmic foci. Red arrows indicate P-bodies; orange arrows indicate colocalization foci.

Supplemental Figure S11

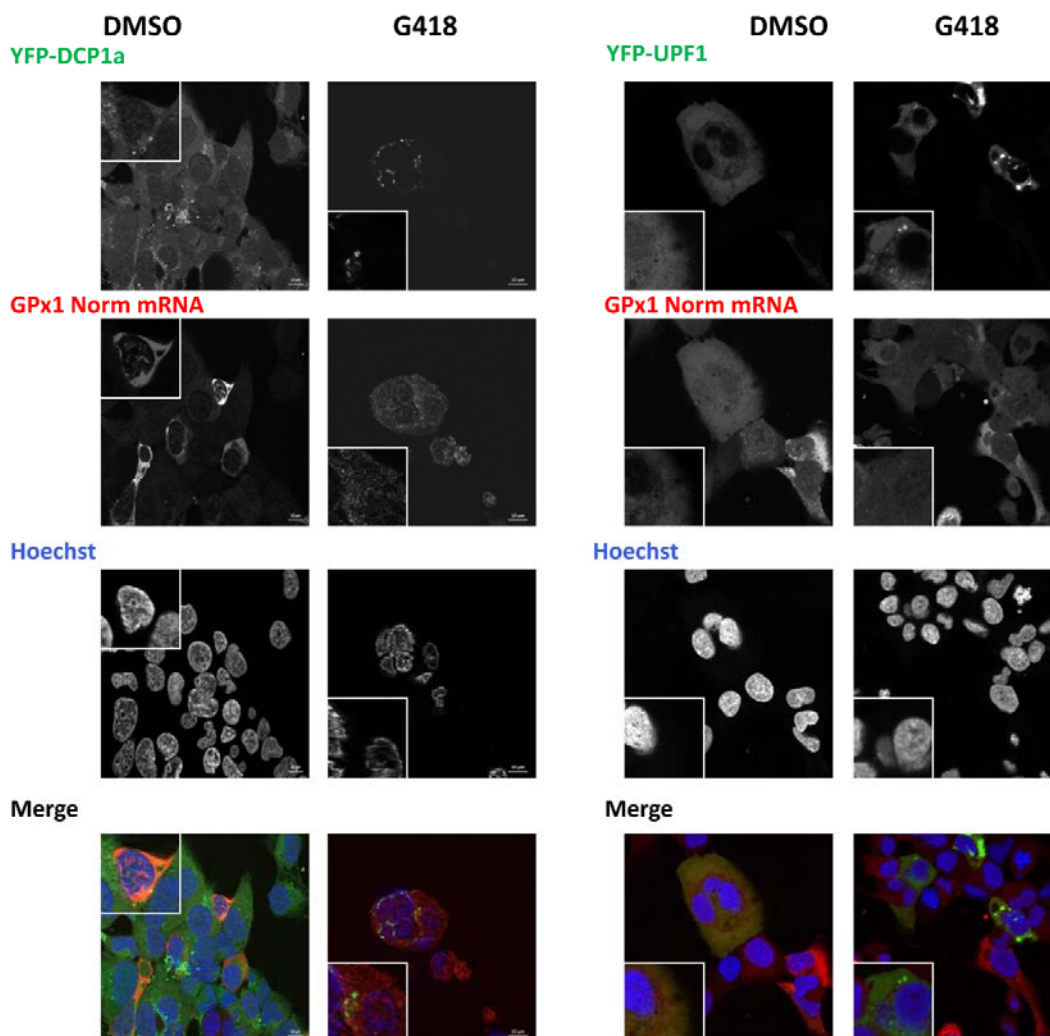
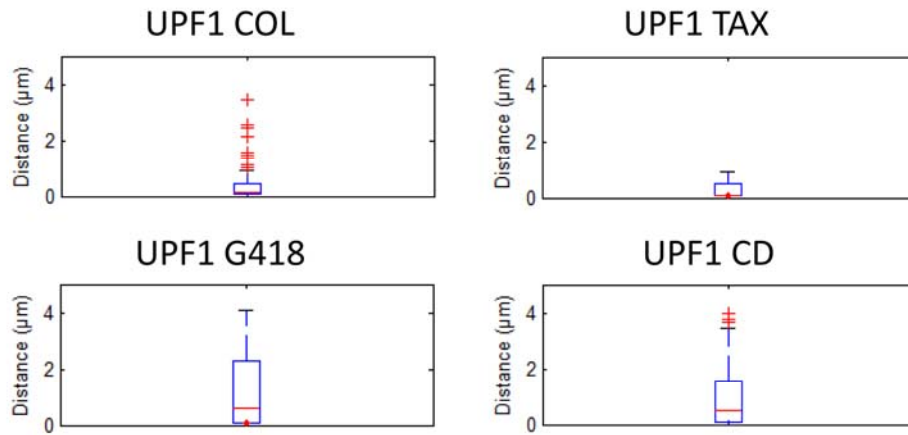


Figure S11: Wild-type GPx1 mRNA does not concentrate in readthrough bodies under G418 treatment. 6CFSMEo- cells were transfected with pCMV-GPx1 Norm and a construct expressing *YFP-DCP1a* (left panels) or *YFP-UPF1* (right panels) before treatment of cells for 48 hours with G418.

Supplemental figure S12

A.



B.

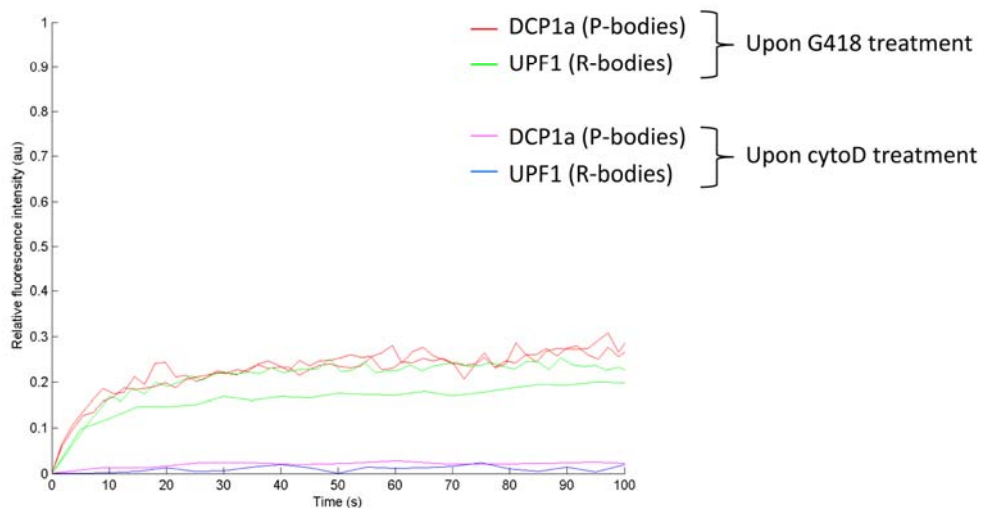
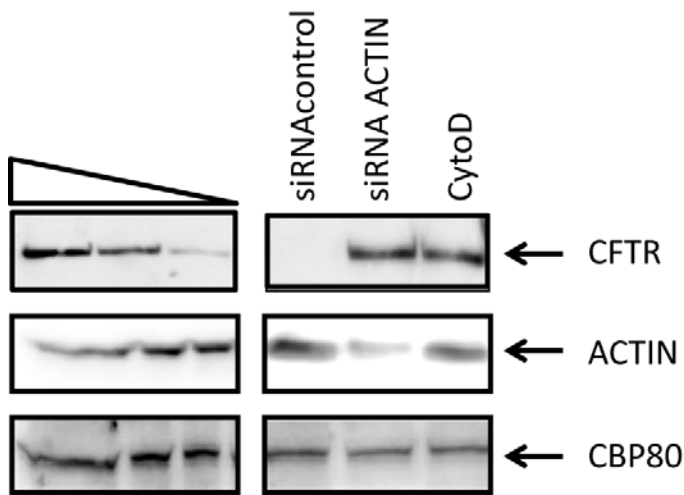
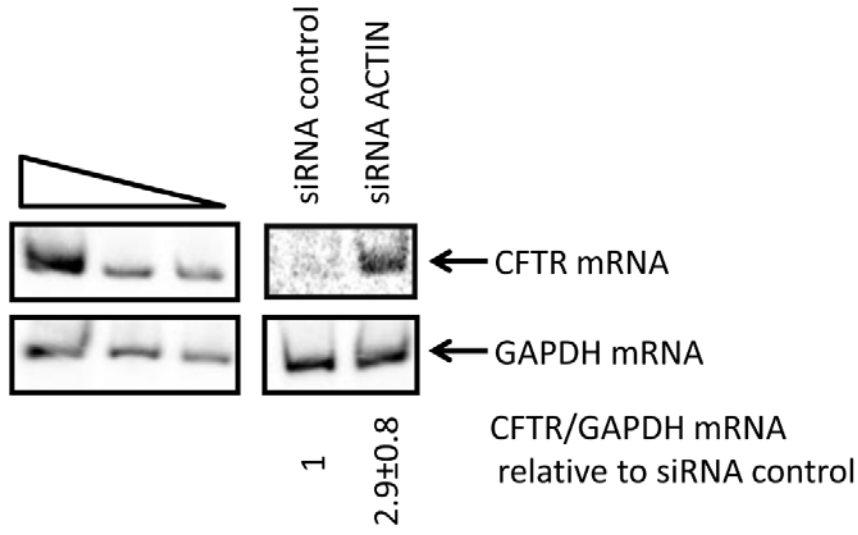
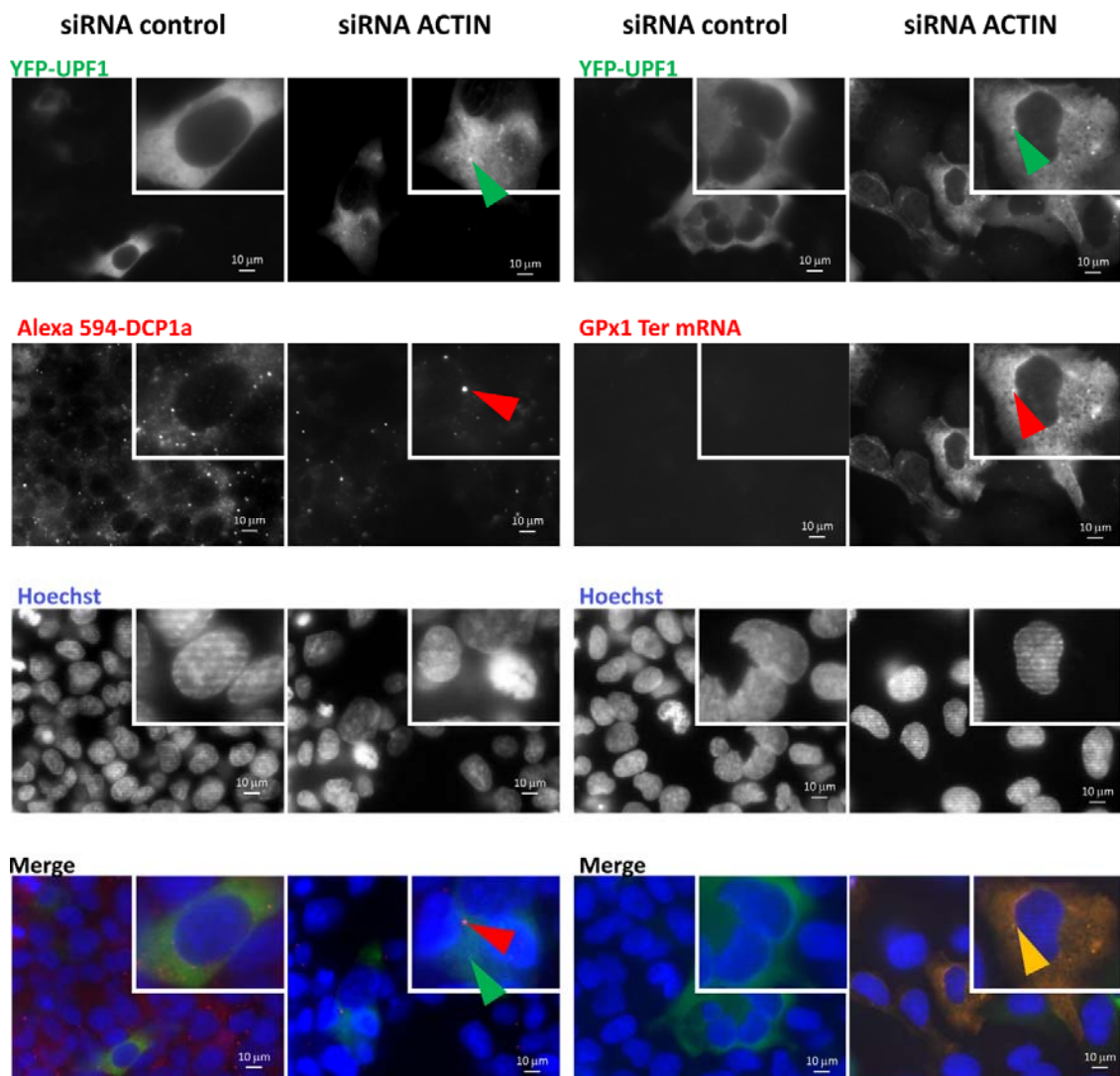


Figure S12: Characterization of readthrough bodies. (A) Measure of the distance between P-bodies and readthrough bodies. Using ImageJ software, distances of P-bodies (DCP1a staining) from a readthrough body were measured in concentric areas centered on that readthrough body (no overlap between UPF1 staining and DCP1a staining) and represented on a boxplot. The measurement was performed with from 5 to 76 readthrough bodies from 6CFSMEo- cells treated with colchicine (COL), Taxotere (TAX), G418 or cytochalasin D (CytoD). (B) Dynamics of readthrough bodies (R-bodies). 6CFSMEo- cells were transfected with *YFP-UPF1* and *RFP-DCP1a* constructs before exposure to cytochalasin D (CytoD) or G418 to induce readthrough body formation. A FRAP assay was then performed to measure the dynamics of readthrough bodies as compared to P-bodies. Upon cytochalasin D treatment, no fluorescence recovery was observed for P-bodies (purple line) or readthrough bodies (blue line). Upon G418 treatment fluorescence recovery was observed and measured for two P-bodies (red lines) and for two readthrough bodies (green lines).

Supplemental figure S13A

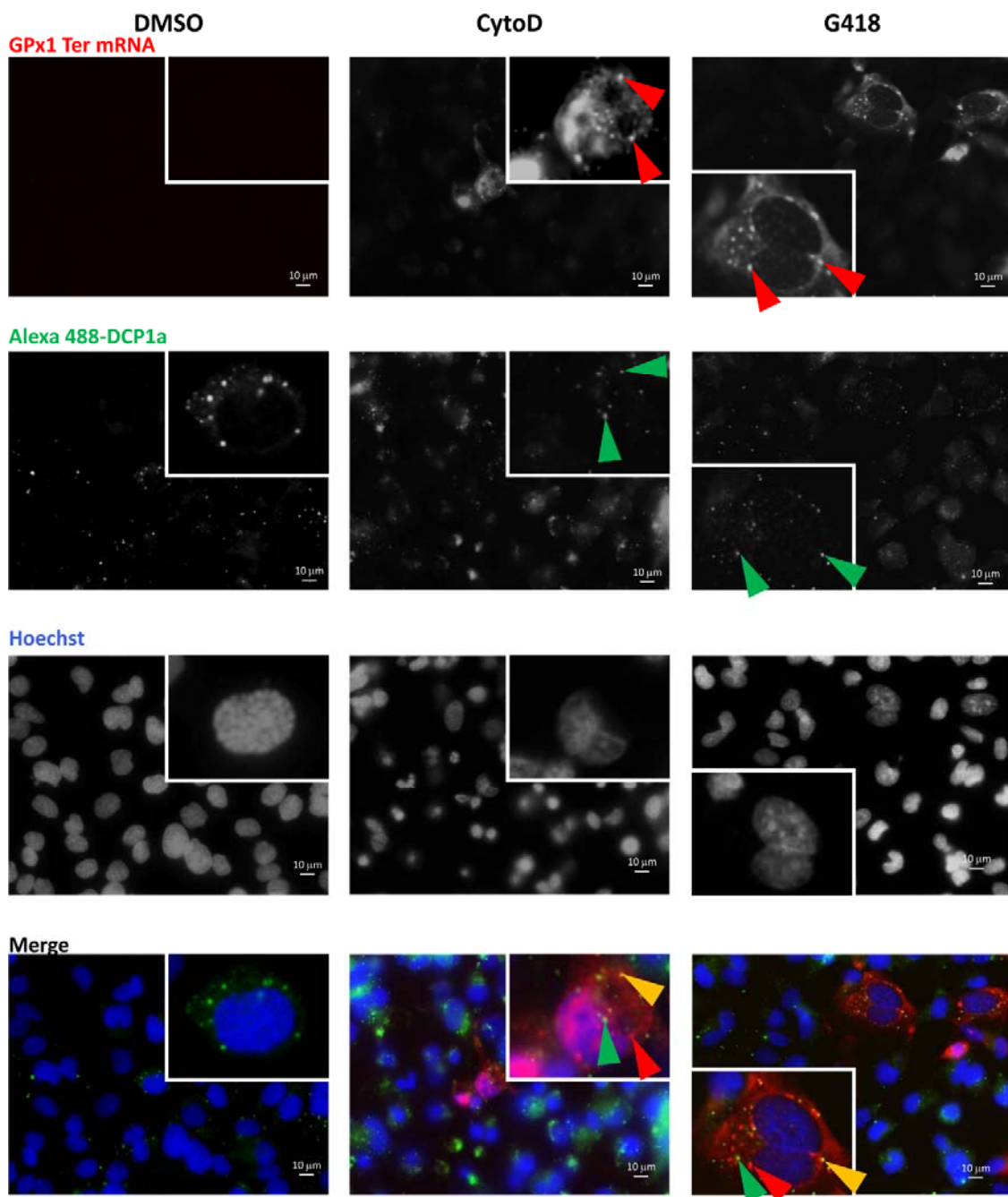


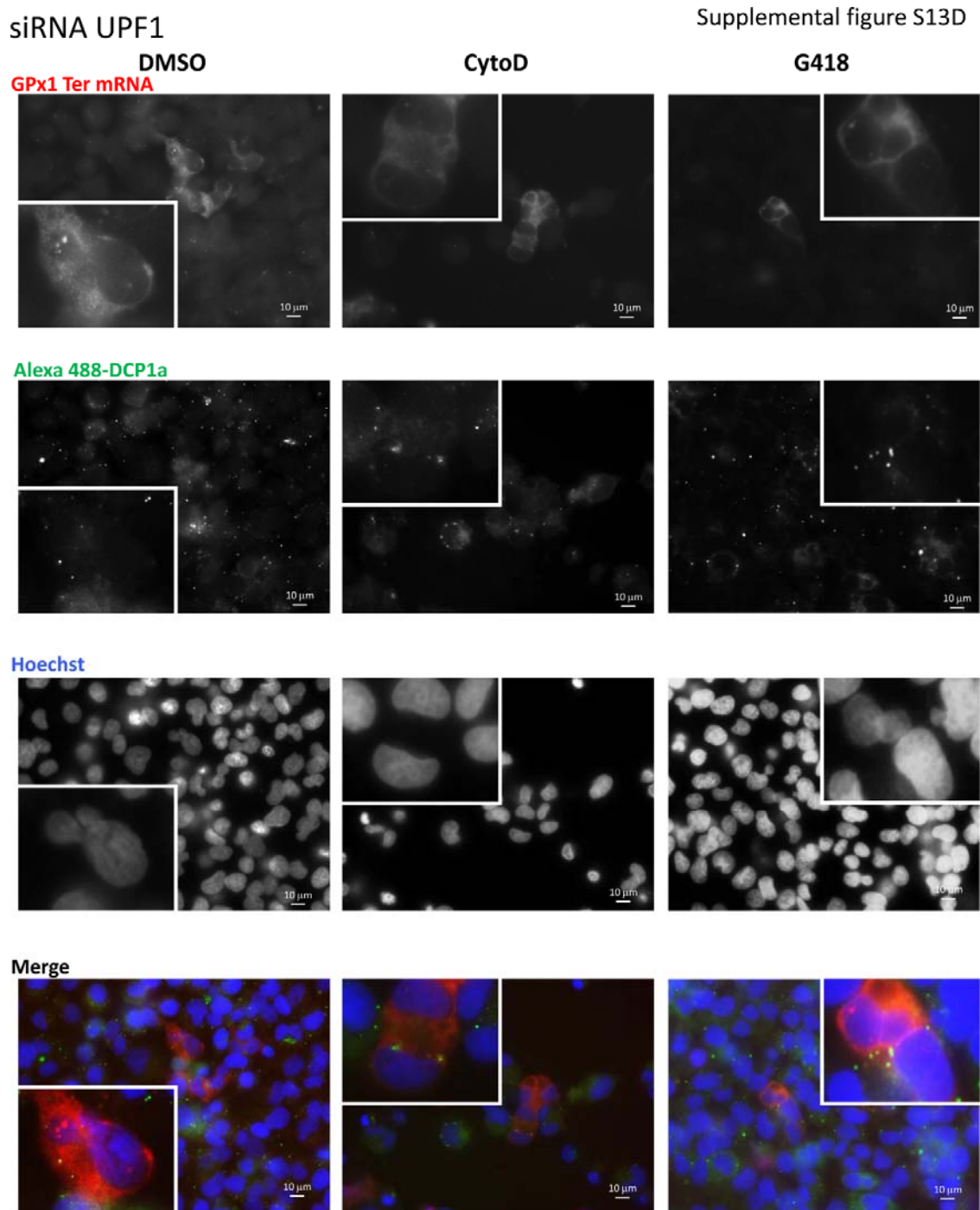
Supplemental figure S13B



siRNA control

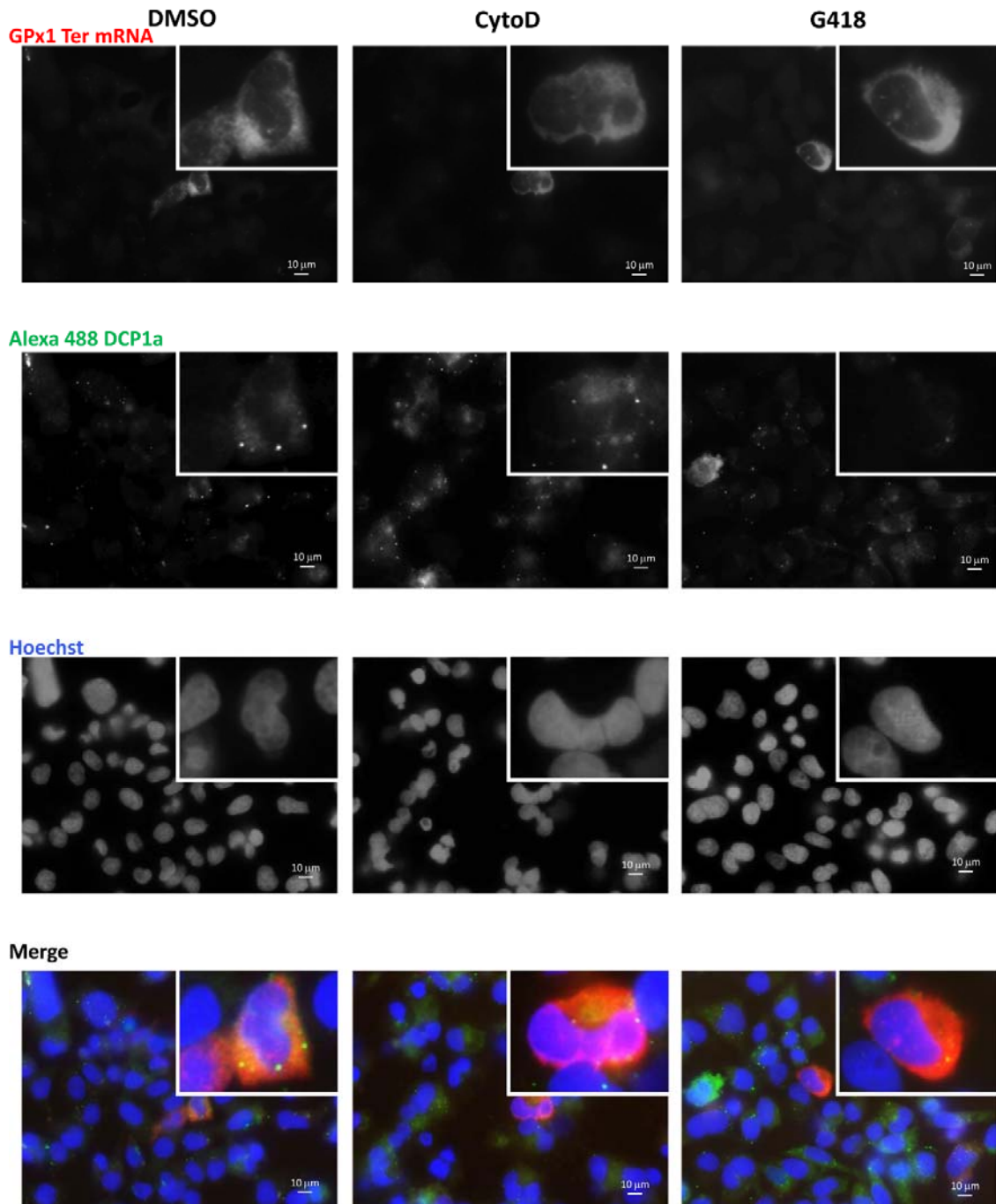
Supplemental figure S13C





siRNA UPF2

Supplemental figure S13E



Supplemental figure S13F

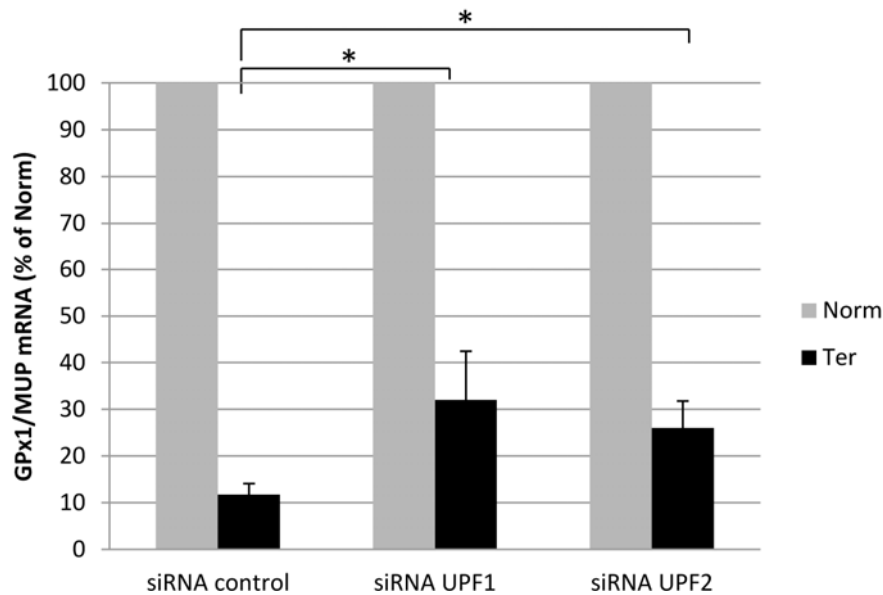
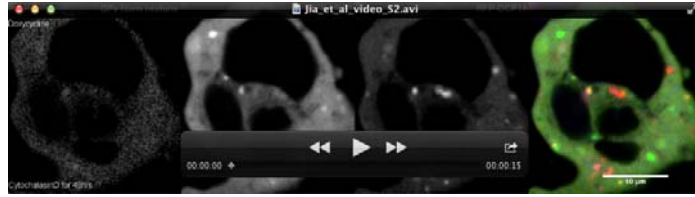


Figure S13: Identification of factors affecting readthrough. (A and B) Actin downregulation inhibits NMD and activates readthrough in 6CFSMEo- cells. (A) The level of CFTR mRNA increased after downregulation of actin, as compared to the level measured in cells transfected with a control siRNA (upper panel). Concomitantly with the inhibition of NMD, readthrough is activated when actin is downregulated as observed by Western-blotting to detect CFTR protein (lower panel). (B) Cytoplasmic foci containing UPF1 or GPx1 Ter mRNA and excluding DCP1a are observed after downregulation of actin. (C-F) The novel cytoplasmic foci are not detected when UPF proteins are downregulated. 6CFSMEo- cells were transfected with pCMV-GPx1 46Ter and (C) siRNA control or siRNA UPF1 (D) or siRNA UPF2 (E). Twenty-four hours after transfection, they were incubated with DMSO, 1 μ M CytoD, or 400 μ g/ml G418 for 48 h. After fixation and permeabilization, cells were incubated overnight at 37°C with Cy3-red-labeled probes. They were then incubated with anti-DCP1a primary antibody followed by Alexa Fluor 488 labeled secondary antibody (green). Nuclei are stained with Hoechst solution (blue). Green arrows indicate P-bodies; red arrows indicate GPx1 mRNA cytoplasmic foci; orange arrows indicate colocalization of P-bodies and GPx1 mRNA. (F) twenty-four hours after transfection with siRNA, cells were divided and transfected with a plasmid encoding MUP mRNA and a plasmid encoding YFP-GPx1 Norm or YFP-GPx1 46Ter. After 48 h, the cells were collected and their RNA was extracted. The levels of GPx1 and MUP mRNA were quantified by RT-PCR. The level of GPx1 mRNA was normalized to the level of MUP mRNA. Error bar=SD, Student's t-test: *=p<0.1.



Movie 1: Readthrough occurs in cytoplasmic foci containing UPF1 but devoid of DCP1a. The experimental procedure is described in the legend of Figure 8. The cellular localization of YFP-UPF1 is in white/green, that of RFP-DCP1a is in white/red and that of GPx1-Neptune is in white/blue. Blue arrows indicate positions of newly synthesized readthrough GPx1-Neptune, green arrows indicate UPF1-containing cytoplasmic foci, and red arrows show DCP1a-containing cytoplasmic foci (P-bodies).



Movie 2: Translation of wild-type mRNA is not confined to readthrough bodies. The experiment was performed as for Video S1 except for the use of an expression construct encoding wild-type GPx1-Neptune mRNA without any PTC. No Neptune signal is found in UPF1 (green) or DCP1a (red) foci under cytochalasin D treatment.



Movie 3: Readthrough does not occur when translation is inhibited. The experiment was performed as for Video S1 except for cells were treated with cycloheximide for 4 hours before to initiate the transcription of Neptune-GPx1 Ter RNA by doxycycline.